The Pennsylvania State University

The Graduate School

Department of Veterinary and Biomedical Sciences

IMINOSUGARS WITH ENDOPLASMIC RETICULUM α-INHIBITOR ACTIVITY ARE POTENT INHIBITORS OF ZIKA VIRUS REPLICATION IN VITRO

A Thesis in

Pathobiology

by

Gitanjali Latha Bhushan

Submitted in Partial Fulfillment
of the Requirements
for the Degree of

Master of Science

December 2018

The thesis of Gitanjali Latha Bhushan was reviewed and approved* by the following:

Suresh V. Kuchipudi
Clinical Associate Professor
Section Head of Mammalian Virology, Immunology and Avian Influenza
Thesis Advisor

Anthony P. Schmitt
Professor of Molecular Virology
Director of Pathobiology Graduate Program

Troy C. Sutton
Assistant Professor of Veterinary and Biomedical Sciences

Santhosh Girirajan
Associate Professor of Biochemistry and Molecular Biology
Associate Professor of Anthropology

*Signatures are on file in the Graduate School

Abstract

Zika virus (ZIKV) is a vector-borne virus of the family *Flaviviridae*, which continues to spread and remains a major global public health threat. Currently, there are no approved vaccines or antivirals against ZIKV. In this study, the anti-ZIKV ability of four iminosugars with endoplasmic reticulum α- glucosidase inhibitor (ER-AGI) activity namely, deoxynojirimycin (DNJ), N-nonyl deoxynojirimycin (*NN*-DNJ), castanospermine and celgosivir were investigated. None of the four ER-AGIs showed any significant ($p>0.05$) cytotoxicity in Vero and human microglia (CHME-3) cells from 0.01 μM to 100 μM concentrations. Iminosugar treatment of Vero or CHME-3 cells infected with ZIKV at a MOI of 0.5 or 5 resulted in significant inhibition of ZIKV replication and the reduction in ZIKV replication was not associated with any significant change in the expression levels of key antiviral genes. Iminosugars protect cells from ZIKV cytopathogenicity as iminosugar treated Vero and CHME-3 cells showed little or no cell death, whereas vehicle control cells exhibited 50-60% cytopathic effect (CPE) at 72 h following ZIKV infection. We further investigated if CPE was the result of apoptosis and/or necrosis. The difference in apoptosis was measured using an activated caspase 3 and 7 assay, and necrosis was evaluated by using a lactate dehydrogenase (LDH) assay in iminosugar treated and control cells following ZIKV infection at a MOI of 1. There was no difference in apoptosis between iminosugar treated and control cells at 48 and 72 hours post infection (hpi). Unlike iminosugars treated cells, untreated control cells exhibited substantial elevation of necrosis at 72 hpi compared with mock-infected cells. In summary, iminosugars with ER-AGI function inhibit ZIKV replication without altering the antiviral gene expression of human cells. The results of this study strongly suggest that ER-AGIs are promising anti-ZIKV antiviral agents and such warrant further *in vivo* studies.

Table of Contents

List of Figures

List of Tables

List of Abbreviations

°C	Degree celsius
BVDV	Bovine viral diarrhea virus
C	Capsid
caspase	Cysteine-aspartic proteases
cDNA	Complementary DNA
Ct	Cycle threshold
DENV	Dengue virus
DMEM	Dulbecco's Modified Eagle Medium
DNA	Deoxyribonucleic acid
DNase	Deoxyribonuclease
DNJ	Deoxynojirimycin
E	Envelope
ER	Endoplasmic reticulum
ER-AGIs	Endoplasmic reticulum alpha glucosidase inhibitors
ERAD	Endoplasmic reticulum associated degradation
FBS	Fetal bovine serum
g	Relative centrifugal force
Gal	Galactose
gDNA	Genomic DNA
h	Hour(s)
HBV	Hepatitis B virus
HCV	Hepatitis C virus
HIV	Human immunodeficiency virus
hpi	Hours post infection
HPRT1	Hypoxanthine phosphoribosyltransferase 1
hpt	Hours post treatment
IFN	Interferon
IRF	Interferon regulatory factor
ISG	Interferon-stimulated gene
JEV	Japanese encephalitis virus
kDa	Kilodalton
LDH	Lactate dehydrogenase
Man	Mannose
MDA5	Melanoma differentiation-associated gene 5
MDMΦ	Monocyte-derived macrophages

mg	Milligram(s)
min	Minute(s)
ml	Milliliter(s)
MOI	Multiplicity of infection
mRNA	Messenger RNA
MTS	3-(4,5-dimethylthiazol-2-yl)- 5-(3-carboxymethonyphenol)-2-(4-sulfophenyl)-2H-tetrazolium
Mx1	Myxovirus resistance protein 1
GalNAc	N-acetylgalactosamine
NADPH	Nicotinamide adenine dinucleotide phosphate
NB-DNJ	N-Butyldeoxynojirimycin
NEAA	Non-essential amino acid
nm	Nanomolar
NN-DNJ	N-nonyl deoxynojirimycin
NS	Nonstructural
p	P-value
PAMP	Pathogen-associated molecular pattern
PBS	Phosphate buffered saline
PrM	Pre-membrane protein
PRR	Pattern-recognition receptor
qPCR	Real-time polymerase chain reaction
REU	Relative equivalent units
RIGI	Retinoic acid-inducible gene I
RNA	Ribonucleic acid
RNase	Ribonuclease
rRNA	Ribosomal RNA
s	Second(s)
SD	Standard deviation
ssRNA	Single stranded RNA
STAT	Signal Transducer and Activator of Transcription
TAM	Tyro3-Axl-Mer receptor family
$TCID_{50}$	50% tissue culture infectious dose
TIM	T-cell immunoglobulin and mucin domain receptor family
TLR	Toll-like receptor
UDP	Uridine diphosphate
UGGT	UDP-glucose:glycoprotein glucosyltransferase
µl	Microliter(s)

μM	Micromolar
WHO	World Health Organization
WNV	West Nile virus
YFV	Yellow fever virus
ZIKV	Zika virus

Acknowledgements

I would like to express my gratitude to my advisor Dr. Suresh V Kuchipudi for allowing me to pursue this Master's and for supporting and mentoring me through this process. Through his guidance, I have been able to appreciate biomedical research to a higher degree. I would like to thank Dr. Tony Schmitt, Dr. Troy Sutton and Dr. Santhosh Girirajan for taking the time to serve on my thesis committee and for providing valuable input during my proposal and thesis meetings.

Thank you to my lab-mates Shubhada, Ian, Levina and Ruth for making me excited to come to the lab every day, welcoming my questions and for valuing scientific curiosity. My friends near and far have invested in my personal and professional goals over the past several years and for that, I am truly grateful. Likewise, Nile, thank you for helping me learn about myself over the last five years.

My family has always encouraged me to learn about myself and the world around me. My dad has guided me through the world of science since I first expressed interest in middle school. My mom has always been there with a smile after a long day in the lab and has been the most positive force. Finally, I would like to thank my sister and best friend for encouraging me to work hard and for always lending an open ear no matter the time or topic.

Chapter 1
Introduction

1.1 Zika virus

1.1.1 History of Zika virus

Zika virus was first discovered in 1947, when a group of researchers conducting routine surveillance for yellow fever isolated a previously unknown virus in a captive, sentinel rhesus macaque. The name Zika comes from Zika Forest (zika meaning "overgrown" in the Luganda language) in Entebbe, Uganda where the rhesus macaque was captured. The macaque developed a fever and an infectious agent was isolated from its serum which is now called Zika virus (1). In 1952, Zika virus was isolated from its first human host in Uganda (2). From its initial discovery until 2007, Zika virus infections were rare. In 2007, large outbreaks occurred in Southeast Asia. Several months later, Zika was confirmed to be the cause of the outbreak (3). The virus then quickly spread throughout the Americas causing more severe symptoms that had not been reported at the time of its discovery (4, 5).

1.1.2 Timeline of Zika virus global spread

Following its initial isolation from the rhesus macaque in 1947, the following year Zika virus was isolated from the *Aedes africanus* mosquito in the Zika Forest (6). In 2007, an outbreak occurred on Yap Island in the Federated States of Micronesia which was the first outbreak to occur outside the African and Asian continents. From 2007 to early 2013 there were no reported seropositive cases in humans. However, in late 2013, an outbreak

occurred in French Polynesia and in the following two years, the virus spread from French Polynesia to the Cook Islands, New Caledonia, Easter Island and other areas in the Pacific region (7). In May 2015, Brazil confirmed its first positive Zika virus case. It is speculated that the virus gained entry into Brazil during the 2014 FIFA World Cup or the World Sprint Championship canoe race which included participants from four Pacific countries. The strain in Brazil was found to be phylogenetically similar to the 2013-2014 strain from French Polynesia, confirming that Zika virus had spread from Pacific countries (8). Following the outbreak in Brazil, Zika virus gained global attention. On February 1, 2016, the World Health Organization (WHO) declared Zika virus a Public Health Emergency of International Concern; the virus had been reported in over 20 countries and territories in the Americas (9). Zika virus has since been linked to infant microcephaly and Guillain-Barré syndrome. However, prior to the 2015 outbreak in Brazil, Zika-associated cases were considered rare and mild (10). Since late 2015, the number of cases of both infant microcephaly and Guillain-Barré has increased which has raised serious concern in health officials and the general public. In 2017, 452 cases of symptomatic Zika virus disease cases were reported in the United States. A majority of these cases were in travelers returning from affected areas. 7 cases were acquired through presumed mosquito-borne transmission and 8 were acquired through other routes such as sexual transmission and laboratory transmission. Additionally, 666 Zika virus disease cases were reported in US territories. 665 of these cases were acquired from presumed local mosquito-borne transmission (11). In 2018, 46 cases of Zika virus disease was reported from travelers returning from affected areas and 98 cases were reported in the US territories, all of which were acquired through

presumed local mosquito-borne transmission (12). No local mosquito-borne Zika virus transmission has been reported in the continental US in 2018. However, Zika virus is still a threat internationally and continues to circulate in the Caribbean, Mexico, the Pacific Islands and many countries in Africa, Asia, Central America and South America. There are areas with interrupted transmission which means that Zika virus was previously found in these locations, but it has been determined that the virus is no longer present. These areas include American Samoa, the Bahamas, Cayman and Cook Islands, Guadeloupe, French Polynesia, Isla de Pascua, Chile and the Marshall Islands (13).

1.1.3 Structure and organization of ZIKV

Zika virus (ZIKV) is an icosahedral, enveloped 10-kilobase, single-stranded RNA virus of the *flaviviridae* family and flavivirus genus. Its genome consists of a linear positive-sense RNA encoding one polyprotein in a single, long open reading frame. The polyprotein is cleaved into individual proteins which consist of three structural and seven non-structural proteins. Structural proteins are encoded at the 5' end of the genome and nonstructural proteins at the 3' end (14). ZIKV structure and genome organization is shown in Figure 1-1 (15).

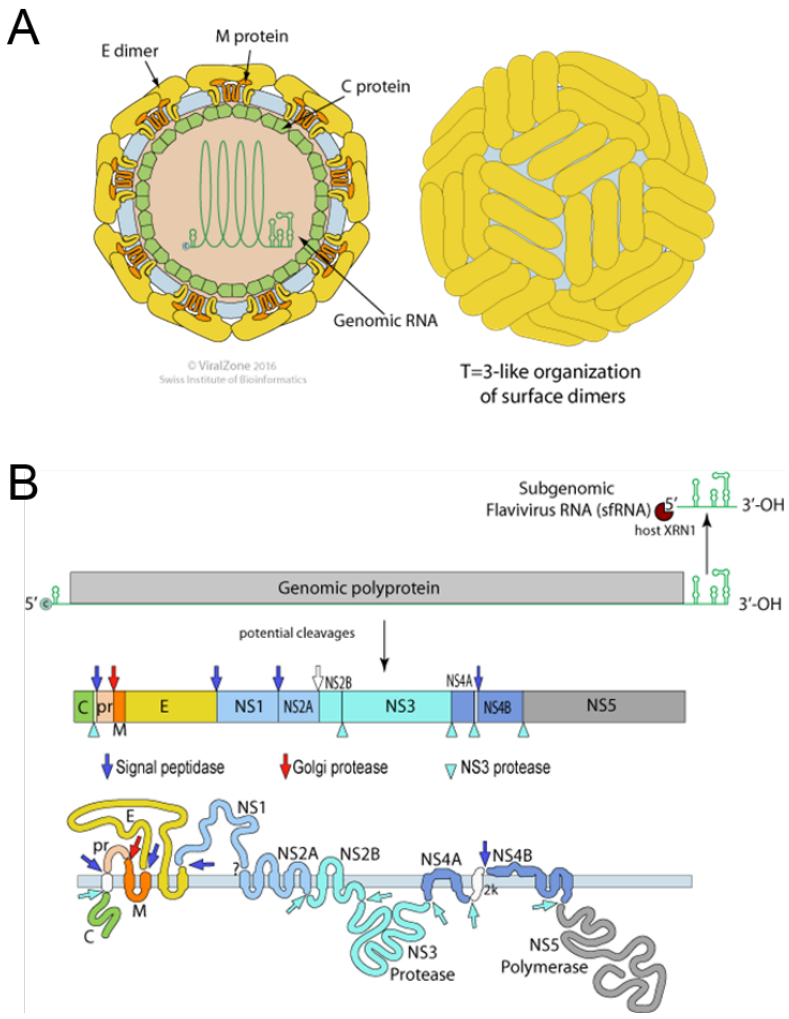

Figure 1-1 ZIKV virion structure and genome organization

Schematic diagram showing **A)** the structure of the ZIKV virion that is enveloped and 50 nm in diameter. The capsid proteins form an icosahedral capsid shell shown in green. **B)** Zika viral genomic polyprotein that is cleaved by viral and host proteases into 3 structural and 7 nonstructural proteins.

Permission to use image granted by SIB Swiss Institute of Bioinformatics, ViralZone (12).

1.1.4 Role of ZIKV proteins

The three structural proteins include the capsid protein (C), premembrane/membrane (PrM) and the envelope protein (E). These three proteins are responsible for maintaining the structural integrity of the virion as well as preventing degradation of viral RNA and other viral components. The capsid protein binds to viral RNA during the process of nucleocapsid assembly which forms the core of mature virus particles (16). The membrane surrounds the envelope protein and prevents its degradation during virion assembly. The premembrane is cleaved to a mature membrane form by a furin enzyme (14). The E protein is responsible for many functions including host cell attachment and entry, membrane fusion and virus assembly. It is also the primary target of neutralizing antibodies in the host (17).

Most nonstructural proteins localize to the endoplasmic reticulum membrane to form the replication complex. NS1 is involved in viral replication and pathogenesis. Additionally, NS1 is responsible for immune evasion by targeting molecules downstream of Toll-like receptor 3 (TLR3). NS2A is also involved in immune evasion by antagonizing the interferon-α (IFNα) and interferon-β (IFNβ) host responses. NS4B also inhibits the IFNα/β pathway by inhibiting host STAT1 phosphorylation and nuclear translocation. Additionally, NS4B is responsible for inducing ER-derived vesicle formation (18). NS3 and NS5 are important pieces to the replication complex as they contain catalytic activity. NS3 is a serine protease that is responsible for post-translationally cleaving the polyprotein. NS2B is critical for NS3's full protease activity.

NS3 also has helicase activity, as it is responsible for unwinding the RNA during the time of replication. NS4A regulates the ATPase activity of the NS3 helicase.

Due the positive-sense nature of the genome, negative-sense anti-genomes are produced using the virus-encoded NS5 protein which is an RNA-dependent RNA polymerase. NS5 also contains methyltransferase activity responsible for 5'capping of the viral genomic RNA. This methyltransferase activity is a necessary step in viral replication. NS5 is also important in the evasion of host immune responses by inhibiting IFN signaling by binding and degrading STAT signaling molecules (19). The anti-genome template produced by NS5 is then used to generate the viral genomic RNA (20). Zika virus proteins and their functions are shown in Table 1-1.

Table 1-1 Zika virus proteins and their functions

	Protein	Encoded protein length in amino acids	Protein Function
Structural	C	122	Encloses nucleic acid and prevents digestion
	PrM	178	Prevents E degradation during virion synthesis
	E	500	Host cell attachment, entry, membrane fusion and virus assembly
Non-structural	NS1	342	Targets TLR3
	NS2A	226	Interferon antagonist protein
	NS2B	130	Regulates NS3 serine protease activity
	NS3	617	Serine protease and helicase activity
	NS4A	127	Regulates NS3 ATPase activity
	NS4B	252	Inhibits STAT1 phosphorylation and nuclear translocation
	NS5	902	RNA dependent RNA polymerase and methyltransferase activity

1.1.5 Replication of ZIKV

Zika virus binds to a proposed set of host cell receptors which include T-cell immunoglobulin and mucin domain (TIM) and tyrosine-protein kinase receptor TYRO3 (TYRO-3), AXL receptor tyrosine kinase (AXL) and Mer proto-oncogene tyrosine kinase (MERTK) (TAM) families of host cell receptors (21). Binding of the virus to host cell receptors leads to clathrin-mediated endocytosis. Once the virus is in the endosome, the endosome undergoes acidification which triggers a conformational change in the glycoproteins of the virion and subsequent virus disassembly. The fusion of the viral membrane and the endosomal membrane allows for the release of the positive-sense viral genome into the cell cytoplasm. ZIKV RNA acts as a template to generate negative-strand viral RNA from which positive-strand RNA is synthesized. This positive-sense mRNA is used to synthesize viral proteins. Flaviviruses replicate exclusively in the cytoplasm on a virus-induced ER-associated network of membranes although Zika virus antigens have also been identified in the nucleus (22, 23). Once the RNA genome is in the cytoplasm, it is translated into one polyprotein that is then cleaved by viral and host proteases into individual viral proteins. Both the viral genome synthesis and protein translation occurs on these ER-associated membranes. Viral components such as viral proteins and positive-sense viral RNA subsequently assemble at the cytoplasmic side of the endoplasmic reticulum membrane. At the ER, viral proteins are processed allowing glycosylated proteins to obtain their mature form. Once assembled, immature virions then bud into the lumen of the endoplasmic reticulum and

are trafficked through the trans-Golgi-network to undergo virus maturation. In the final moments before the virus is secreted from the cell, prM undergoes furin cleavage to produce M and Pr peptides. The neutral environment of the extracellular matrix allows Pr to dissociate from M allowing the virus particle to finally become fully mature (24). The replication cycle of Zika virus is shown in Figure 1-2 (25).

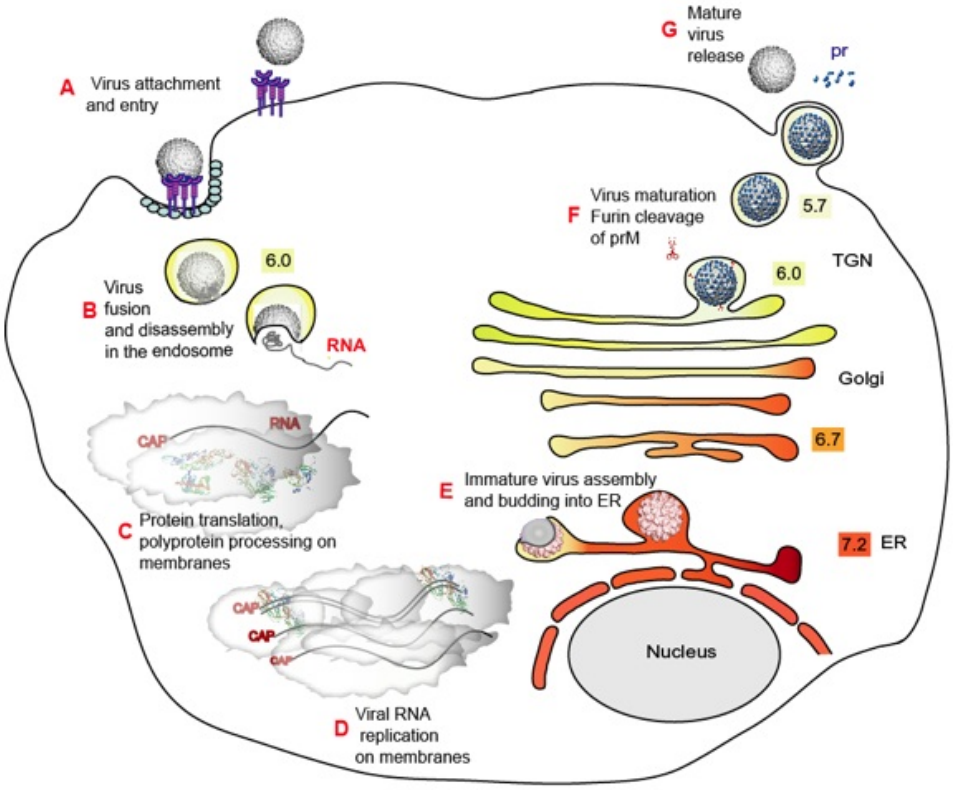

Figure 1-2 Zika virus replication cycle

Illustration describing the stages of ZIKV replication. **A)** ZIKV first binds to host cell receptors and enters the cell through clathrin-mediated endocytosis, **B)** Endosomal acidification and virus disassembly, **C)** Polyprotein translation, **D)** Viral RNA replication, **E)** Immature virus assembly and budding into the ER, **F)** Virus maturation and furin cleavage of prM and **G)** Mature virus release

Permission to use image granted by Richard J. Kuhn, Purdue University (25).

1.2 **Epidemiology of ZIKV**

1.2.1 Vectors

Zika virus is classified as an arbovirus which means that it is transmitted by arthropods such as mosquitos that act as asymptomatic vectors of ZIKV and transmit the virus by biting the next amplifying host. Routes of transmission to humans other than mosquitoes include sexual intercourse, perinatal transmission, blood transfusion and laboratory exposures (26). The primary arthropod vectors of ZIKV are from the *Aedes* family. ZIKV was first isolated from *Aedes africanus* in 1948 and has been since isolated from *Aedes aegypti* and *Aedes albopictus* which are confirmed competent vectors for ZIKV transmission (5).

After *Ae. Africanus, Aedes aegypti* was the next mosquito that ZIKV was isolated from in Malaysia in 1966 and was the first vector found to be competent for ZIKV. It is present in tropical and subtropical areas of America, Africa, Asia and Oceania. It may colonize southern Europe and Northern America in the near future as the temperatures begin to rise in the northern hemisphere (27). *Ae. aegypti* breeds in both indoor and artificial outdoor containers that contain clean water with low salt and organic content. These mosquitos need only a shallow area to breed which allows them to exist in many containers and environments. However, its activities are inhibited under 14 ºC and deposition of eggs is inhibited lower than 17 ºC. *Ae. aegypti* prefer to feed on humans domestically and do not stray from their breeding sites (28).

The second vector which has been involved in the largest Zika virus outbreaks is *Aedes albopictus. Ae. albopictus* bites humans, domestic animals and livestock in outdoor

environments. It is present in tropical, subtropical and temperate climates and has spread from Asia to the South Pacific, Africa and Europe as well as Brazil and the Dominican Republic (28). *Ae. albopictus* was first recorded in Brazil in 1986 and has now colonized 20 of 27 Brazilian states. It breeds in various water-filled sites and is abundant in rural, peri-urban and now urban environments. It also prefers to feed on humans but takes a large proportion of blood meals from birds (29). Its eggs are resistant to cold and its optimum water temperature is 25 ºC (28). *Aedes albopictus* are opportunistic and invasive when *Aedes aegypt*i is absent (23).

1.2.2 Host range

Zika virus's ability to rapidly spread maybe be in part due to its capacity to exist in sylvatic and urban cycles. The sylvatic cycle is the proportion of time the virus spends circulating between wild animals and mosquito vectors. The sylvatic cycles have existed for years between non-human primates and arboreal mosquitos in tropical areas of Africa (30). An urban cycle is when the virus cycles between mosquito vectors and urban or domestic animals. In the urban cycles, humans are the primary amplification hosts whereas in sylvatic cycle, non-human primates are the amplifying hosts (23). ZIKV antibodies have also been detected in sheep, goats, horses, ducks, rodents, bats, orangutans and carabaos (5).

1.3 **ZIKV infection**

1.3.1 Pathogenicity of ZIKV

The majority of clinical Zika virus infections are asymptomatic (80%). However, when symptoms are observed they are similar to other flaviviruses such as Dengue virus (DENV), West Nile virus (WNV) and Yellow virus fever (YVF) which all produce nonspecific symptoms such as arthritis, fever, conjunctivitis, myalgia, retro-orbital pain, mild gastrointestinal disorder and headache (31).

In addition to these symptoms, maculopapular rash is usually observed in Zika virus infection. The infection itself is self-limited and only lasts a few days. Its incubation time is estimated to be 3 to 14 days with 50% of those infected developing symptoms within one week and 99% of those infected developing symptoms within 2 weeks (32).

Since its emergence in the Americas, ZIKV has been associated with increased infection rates and neurological pathologies such as Guillain-Barre syndrome, microcephaly, meningoencephalitis and myelitis. Guillain-Barre syndrome (GBS) is an autoimmune disorder in which the immune system attacks the myelin sheath of nerves in the peripheral nervous system (PNS). Some of these syndromes include acute inflammatory demyelinating polyneuropathy (AIDP), acute motor axonal neuropathy (AMAN), acute motor sensory axonal neuropathy (AMSAN) and Miller Fisher syndrome (MFS). Symptoms begin with paralysis and can then become fatal if no intervention is provided (33). It has been suggested that microcephaly is caused by direct ZIKV infection in the brain of fetuses which is also termed as viral pathology (34). Microcephaly is a condition in which fetuses are born with small heads due to abnormal brain development.

Problems with microcephaly include intellectual disability, speech delay and abnormal muscle functionality (14). ZIKV RNA has been found in amniotic fluid as well as the brain of fetuses and infants with microcephaly. It has also been established that microcephaly has been linked to maternal ZIKV infection due to the high rate of microcephaly among infants born to ZIKV-infected mothers (35). It has been shown that ZIKV crosses the placenta and that the placenta is the key mediator of vertical transmission from mother to fetal brains. Zika virus reaches the fetus by infecting placental cells and disrupting the placental barrier and causing placental damage (36). In addition to placental cells such as Hofbauer macrophages and trophoblasts, other brain cells are targets of ZIKV infection (37). *In vitro* studies have shown that neural progenitor cells (NPCs) are vulnerable to ZIKV infection (38). Additionally, astrocytes, microglia and oligodendrocyte precursor cells that are in the developing cortex can be infected by ZIKV. Glial cells have been shown to be important for normal brain development (39). The disruption of these cells by ZIKV infection may therefore contribute to the neurodevelopmental disorder that is seen in microcephaly.

1.3.2 Pathogenesis

Currently, there is only one serotype of Zika virus, but phylogenetic analyses show two lineages, one African and the other Asian. Phylogenetic analysis revealed epidemic ZIKV strains from the Americas clustered together with the Asian lineage of Zika virus, indicating a closer relationship to Asian lineages than African lineages. African strains have been shown to induce more cytopathic effect *in vitro* in comparison to Asian strains.

It is speculated that Asian strains induce less cytopathic effect to allow more pathogenesis while continuing virus replication and maintaining cell viability (40). Comparison of pre-epidemic and epidemic strains of Zika virus has shown many amino acid substitutions among epidemic strains which may be responsible for the increased neuropathogenicity (41).

1.3.3 Host response to ZIKV

The interferon (IFN) pathway is an important component of the innate immune system that helps the host fight viral infection. Viruses are recognized by their viral pathogen-associated molecular patterns (PAMPs) such as viral RNA and are sensed by cellular pathogen-recognition receptors (PRRs) that are located on the cell membrane and within the cytoplasm (MDA5 and RIGI). Once the virus is sensed, the pathway ultimately allows for transcription and secretion of Type I IFNs (IFNα/β). Type I IFNs bind to neighboring cells to stimulate the transcription of IFN-stimulated genes (ISGs) which then limit viral replication (42). ZIKV's structural and non-structural proteins have been implicated in the evasion of host Type I IFN response as described earlier in Table 1-1 and section 1.1.4 and contribute to ZIKV's ability to maintain infection in cells (20).

1.4 **Prevention and control of ZIKV infection**

Prevention and control of Zika virus has been approached from two main angles: vector control and symptomatic therapy. Although both approaches have been important in reducing ZIKV spread and ZIKV-induced suffering, both approaches have their limitations in blocking ZIKV transmission and mitigating disease associated with ZIKV.

Currently, there is an urgent need to develop effective prophylactic and therapeutic agents for ZIKV infection.

1.4.1 Vector control

To-date, traditional vector control practices such as use of outdoor fogging with insecticides, insecticide-treated materials at home, such as mosquito nets and medicated topical applications are widely used to control malaria and other mosquito-borne viral diseases including Zika virus. However, the effect of vector control practices is short-lasting and its effects can be compromised by the spread of mosquitoes resistant to insecticides (43). In recent years, newer approaches such as release of mosquitoes infected with a strain of Wolbachia to block transmission of Dengue, Chikungunya, and Zika viruses is currently being tested in Southeast Asia and in implementation trials that are ongoing against ZIKV in Colombia and Brazil (44).

1.4.2 ZIKV vaccines and antivirals

Despite considerable need for novel vaccines and antiviral therapies, there are no FDA-approved drugs to prevent or treat ZIKV infection.

Many Zika virus vaccines are currently under development. These candidates include inactivated Zika virus, attenuated Zika virus strains, live or inactivated viral recombinants expressing Zika virus proteins, viral-like particles expressing Zika virus membrane proteins, DNA plasmid vaccines, mRNA-based vaccines, protein-nanoparticle conjugates and peptide-based vaccines. Some of these vaccines are in phase I clinical trials whereas others are still in preclinical animal studies. However, the majority of vaccines are

still in the early stages of research (45). Flaviviruses often show antigenic cross-reactivity which share immunogenic epitopes that stimulate immune responses. In many cases cross-reactivity is beneficial to the host. However, antibody-dependent enhancement (ADE) which is caused by preexisting poorly neutralizing antibodies can occur, causing enhanced disease to the host as seen in DENV infection (46). Further vaccine development studies must confirm that this cross-reactivity is protective to make sure vaccines will not exacerbate ZIKV disease.

The search for these antiviral therapies includes looking for novel compounds that target major steps in the Zika virus replication cycle. As of now, ZIKV antiviral research has been directed at virus entry and the virus replication pathway. Virus entry is mediated by a set of proposed receptors such as T-cell immunoglobulin and mucin domain (TIM) and TYRO-3, AXL and MERTK (TAM) families (47). Nevertheless, there may be other receptors that allow for ZIKV recognition and entry, therefore circumventing the blockage of these proposed receptors.

A clinically approved antiviral drug sofosbuvir is currently being examined for its use in ZIKV infection. Sofosbuvir has shown to be effective in another virus within the flaviviridae family, HCV. Sofosbuvir targets a conserved region across flaviviridae viruses which is the RNA polymerase protein, NS5. A pronounced reduction in ZIKV production has been observed upon sofosbuvir treatment in brain organoids and neuronal cell systems (48). Another repurposed drug in development for ZIKV includes favipiravir that also is a nucleoside precursor RNA polymerase inhibitor that been shown to be effective across many RNA viruses. Anti-ZIKV evaluations of favipiravir include using traditional tissue

culture methods, hollow-fiber infection models and mechanism-based mathematical modeling (49).

Virus-directed therapies may lead to drug resistance especially in the case of RNA viruses such as Zika virus that have a high mutation rate. The best antiviral strategy to avoid the evolution of ZIKV would be to use a combination of virus-directed and host-directed antivirals. This thesis examines a host-directed antiviral strategy that targets enzymes located in the endoplasmic reticulum that are necessary for processing of N-glycosylated viral proteins such as ZIKV PrM, E and NS1 proteins.

1.4.2.1 Endoplasmic reticulum α-glucosidase inhibitors as antivirals (ER-AGIs)

Most virus envelopes contain N-linked glycans in their glycoproteins. These glycoproteins undergo maturation in the endoplasmic reticulum. In the case of ZIKV, three viral proteins are N-glycosylated and they include the prM, E and NS1 proteins. These glycoproteins are substrates for the ER α-glucosidase enzymes during ZIKV replication (50).

In normal processes, ER α-glucosidases I and II are responsible for trimming terminal glucose moieties on N-linked glycans attached to nascent glycoproteins. α-glucosidase I removes the outermost α-1,2-linked glucose residue while α-glucosidase II removes the inner two α-1,3-linked glucose residues. These steps are necessary for calnexin/calreticulin chaperone interaction which is critical for proper folding and transport. Incompletely folded proteins are re-glycosylated by UDP-glucose:glycoprotein glucosyltransferase (UGGT) and undergo the process again until they are properly folded.

Properly folded glycoproteins then move to the Golgi apparatus for maturation. Improperly folded glycoproteins will be retained and accumulate in the ER and will ultimately undergo ER-associated degradation (ERAD) (51). The mode of action of ER α-glucosidases I and II enzymes on viral glycoproteins and their inhibition by ER-AGIs are shown in Fig. 1-3.

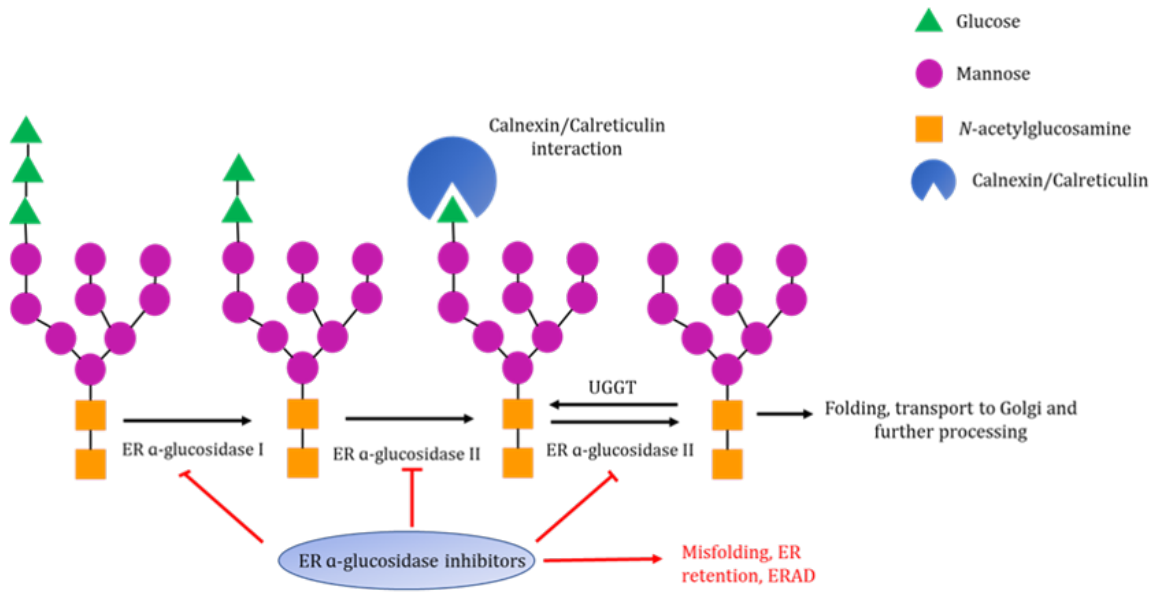

Figure 1-3 Mode of action of ER-AGIs on viral glycoproteins.

Endoplasmic reticulum (ER) α-glucosidase I and II sequentially cleave off terminal glucose moieties on N-glycosylated proteins to allow for subsequent interaction with chaperone proteins, calnexin and calreticulin that are required for proper glycoprotein processing. If glycoproteins are misfolded UDP-glucose:glycoprotein glucosyltransferase (UGGT) re-glycosylate the protein until it is properly folded. Inhibition of endoplasmic reticulum α-glucosidase I and II by endoplasmic reticulum α-glucosidase inhibitors (ER-AGIs) impedes viral glycoprotein maturation and targets proteins for ER-associated retention, accumulation and degradation therefore hampering virus particle maturation and development.

Image adapted from *Chang et. al. 2013*

Flavivirus particles are extremely reliant on ER glucosidases for trimming of their glycoproteins and their following interactions with ER chaperones calnexin and

calreticulin. This antiviral approach has been supported by the observations of significant reduction of DENV, YFV and ZIKV viral replication in Gluc I knockout and Gluc II knockout cell lines in comparison to wild-type cells. This study also showed that ER α Gluc I was more critical in reducing virus replication in comparison to ER α Gluc II (52). Additionally, patients deficient in these enzymes had no clinical evidence of recurrent viral infections and cells derived from these patients were unable to support infection by multiple viruses such as HIV, Influenza, Adenovirus, Poliovirus and vaccinia virus (53, 54).

ER α-glucosidase I and II can be inhibited by iminosugars. Iminosugars are sugar mimetics in which cyclic oxygen is replaced with a nitrogen. They mimic endogenous sugars and compete with endogenous substrates for binding to ER α-glucosidases. The antiviral strategy of targeting ER α-glucosidases with iminosugars has shown to be effective in other flaviviridae infections such as Dengue virus (DENV), Japanese encephalitis virus (JEV), Yellow Fever virus (YFV), Bovine viral diarrhea virus (BVDV) and hepatitis C virus (HCV) (52, 53). Although these antiviral compounds seem to be effective in many flaviviruses and other enveloped viruses, few studies have examined the role of these compounds in ZIKV infection. Some studies have showed that addition of IVHR-19029, a N-alkyl analog of deoxynojirimycin (DNJ) demonstrated broad antiviral efficacies against several hemorrhagic fever viruses *in vitro* and partial protection of EBOV and MARV in an *in vivo* mouse model (55-57). A recent study by Ma *et. al.*, that was published when this study was underway, has shown that an iminosugars, IVHR-19029 is a potent inhibitor of the replication of a range of flaviviruses which include DENV, YFV

and ZIKV by decreasing viral replication and increasing cell viability of HEK 293T cells (52). These results show the promising nature of iminosugars as ER α-glucosidase inhibitors and their promise as antiviral agents against ZIKV. This evidence warrants further studies to investigate the efficacy of mono and bicyclic amines and the differences between the parent and the derivative compounds to inhibit ZIKV replication.

1.5 **Hypothesis**

ER α-glucosidase inhibitors (ER-AGIs) reduce Zika virus replication *in vitro*.

1.5.1 Objectives

1. **To evaluate the cytotoxicity of iminosugars *in vitro.***

To investigate whether iminosugars induce cytotoxicity in either *Flaviviridae* permissive African green monkey kidney cells (Vero) or clinically relevant human microglial cells (CHME-3) using a 3-(4,5-dimethylthiazol-2-yl)-5-(3-carboxymethoxyphenyl)-2-(4-sulfophenyl)-2H-tetrazolium (MTS) assay.

2. **To investigate the role of iminosugars as ER-AGI antivirals in ZIKV-infection *in vitro*.**

To understand whether iminosugars are able to reduce virus replication using real-time polymerase chain reaction analysis (qRT-PCR) and 50% tissue culture infectious dose assay ($TCID_{50}$). Additionally, to study iminosugars role as ER-AGIs and their effect on cellular antiviral gene expression in human microglial cells.

3. To characterize the effect of ER-AGIs on ZIKV cytopathogenicity.

To evaluate ZIKV cytopathogenicity using an MTS assay to study general metabolic activity after ZIKV infection and ER-AGI treatment. Additionally, to investigate cytopathogenicity mechanisms such as apoptosis and necrosis and the effect of ER-AGIs on both mechanisms.

Chapter 2
Materials and Methods

2.1 **Viruses**

Two human ZIKV isolates namely PRVABCB59 (Human/2015/Puerto Rico), IBH30656 (Human/1968/Nigeria) and one mosquito ZIKV isolate MEX 2-81 (Mosquito/2016/Mexico) obtained from BEI Resources (BEI Resources, Manassas, VA) were used in this study. All viruses were propagated in Vero cells and virus titration was carried out by $TCID_{50}$ method in Vero cells (58).

Table 2-1 Viruses used in this study

	Strain lineage	Year	Location	Isolated from	BEI Resources Catalog No.
PRVABC59	Asian	2015	Puerto Rico	Human patient	NR-50240
IBH30656	African	1968	Nigeria	Human patient	NR-50066
MEX 2-81	Asian	2016	Mexico	*Aedes aegypti* mosquito	NR-50280

2.2 **Cell lines**

African green monkey kidney Vero (CCL-81) cells were purchased from ATCC (ATCC, Manassas, VA) and cultured in Dulbecco's modified Eagle's medium (DMEM) (Corning, Corning, NY) supplemented with 10% heat-inactivated fetal bovine serum (FBS) (Corning) and 1% antibiotic/antimycotic solution (Corning) at 37 °C incubator under 5% CO_2. Human microglial cell line CHME-3 was provided by Dr. Pamela Hankey (Penn State University, University Park, PA) and cultured in DMEM (Corning) supplemented with 10% FBS (Corning) and 1% antibiotic/antimycotic solution (Corning) and 0.1% MEM

non-essential amino acids (NEAA) (GE Life Sciences, Marlborough, MA) at 37 °C incubator under 5% CO_2. Medium was changed every three days.

2.3 **Compounds**

Iminosugars, castanospermine, 1-deoxynojirimycin hydrochloride (DNJ) and N-Nonyldeoxynojirimycin (NN-DNJ) were purchased from Sigma-Aldrich (St. Louis, MO), and Celgosivir was purchased from MedChem Express (Monmouth Junction, NJ). Castanospermine, Celgosivir, and DNJ were dissolved in sterile nuclease free water whereas NN-DNJ was dissolved in dimethyl sulfoxide (DMSO). Compounds structures are shown in Figure 2-1. Compound stock volumes and concentrations are shown in Table 2-2.

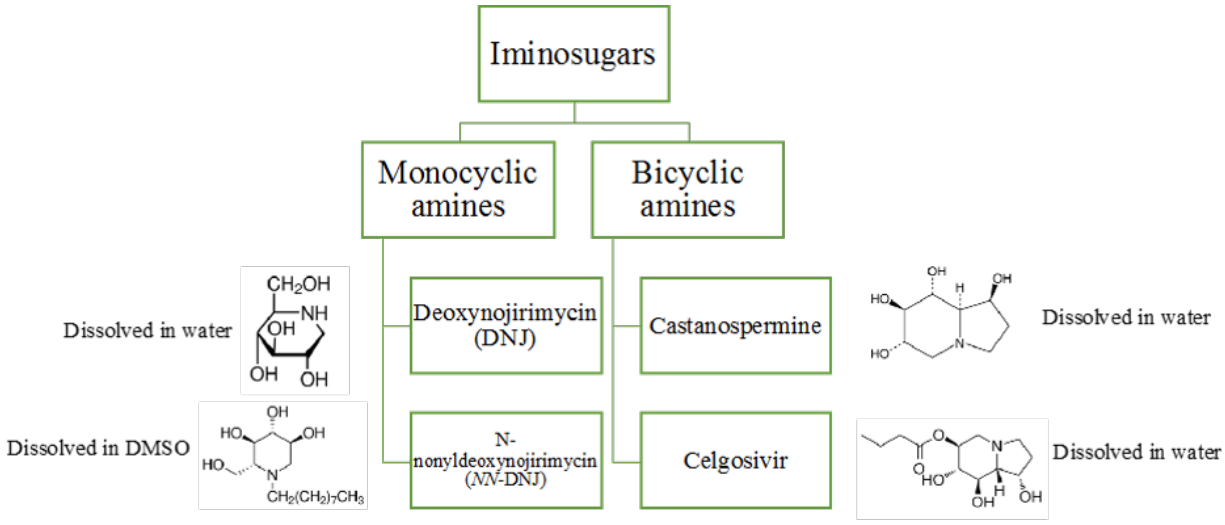

Figure 2-1 Iminosugar structures and solvents

Iminosugars can be subgrouped into monocyclic amines and bicyclic amines. Deoxynojirimycin (DNJ) and its derivate N-nonyldeoxynojirimycin (NN-DNJ) were representative monocyclic amines. Castanospermine and its derivative Celgosivir were representative bicyclic amines. DNJ, castanospermine and Celgosivir were dissolved in water whereas NN-DNJ was dissolved in DMSO. Chemical structures were obtained from manufacturer websites.

Table 2-2 Compound stock volumes and concentrations

Compound		Amount (mg)	Solvent	Molar mass of compound (g/mol)	Stock concentration* (mg/mL) and (μM)	Working concentration (μM)	Volume of stock solution	Supplier and Catalog No.
A	Castanospermine	100	Water	189.21	20 mg/mL 105702.6 μM	1000	33.11	Sigma-Aldrich C3784-5MG
B	Celgosivir	5	Water	295.76	200 mg/mL 676223.9 μM	1000	5.18	MedChem Express HY-16134A
C	DNJ	5	Water	199.63	20 mg/mL 100185.3 μM	1000	34.94	Sigma-Aldrich D9305-5MG
D	NN-DNJ	5	DMSO	289.41	10 mg/mL 34553.0 μM	1000	101.29	Sigma-Aldrich N6414-5MG

*Ideal stock concentration according to manufacturer's protocol

2.4 **General *in vitro* ZIKV infection model**

Cells were washed twice with PBS before infection with Zika virus at various MOI. The infection media for different types of cells are listed in Table 2-3. For antiviral screening and ZIKV cytopathogenicity mechanism assays, cells were incubated concurrently with both virus and compound. For virus quantification and gene expression studies, cells were incubated with ZIKV at 37 °C with 5% CO_2 for 2 h before being washed with PBS and treated with 1 μM of compounds. Supernatants were harvested and centrifuged at 8000 g for 5 min to remove cellular debris. Supernatants were stored at -80 °C until further use.

Table 2-3 The composition of infection medium for cells used in this study

	Cell-type	
	Vero Cells	CHME-3 Cells
Medium	DMEM	DMEM
Supplements	5% fetal bovine serum, 1% penicillin and streptomycin	5% fetal bovine serum, 1% penicillin and streptomycin 0.1% non-essential amino acids

2.5 **High-throughput cytotoxicity and antiviral screening assay**

2.5.1 MTS assay

A cell viability assay was used to initially screen cytotoxicity and determine the effect of ER-AGIs on ZIKV cytopathogenicity. This was carried out by using the 3-(4,5-dimethylthiazol-2-yl)-5-(3-carboxymethoxyphenyl)-2-(4-sulfophenyl)-2H-tetrazolium (MTS) assay which is a colorimetric assay used for assessing a cell's metabolic activity. Cellular NADPH oxidoreductase enzymes are the basis of this assay and reduce tetrazolium dye into insoluble formazan which has a purple color. The intensity of purple color detected through spectrophotometry reflects the number of viable cells present under certain conditions. Therefore, this assay was used to determine the effect of ER-AGIs on ZIKV cell viability.

A cell viability assay previously described by Fletcher et. al. (59), was used. The assay was performed using CellTiter 96® AQueous One Solution Cell Proliferation Assay (MTS) (Promega, Madison, WI) following the manufacturer's instructions. At 60-70% confluence, Vero cells and CHME-3 cells were treated according to the plate layout shown in Figure 2-2. Four biological replicates were used to assess cytotoxicity, and four

replicates were used to assess the effect ER α-glucosidase inhibitors on ZIKV cytopathogenicity with concentrations ranging from 0.01 µM to 1000 µM. Vero cells treated with ER α-glucosidase inhibitors or vehicle control were infected with ZIKV strain PRVABC59, IBH30656 or MEX 2-81 at a multiplicity of infection (MOI) of 1 in infection medium containing DMEM supplemented with 5% FBS, 1% antibiotic/antimycotic solution. CHME-3 infection medium was additionally supplemented with 0.1% NEAA. At 72 h post infection (hpi), MTS solution was added to the wells and after 2 h the optical density was measured at 490 nm using a microplate reader (ELx800; BioTek). Each assay was repeated three times and the data was analyzed using Microsoft Excel and graphed on Prism 7.

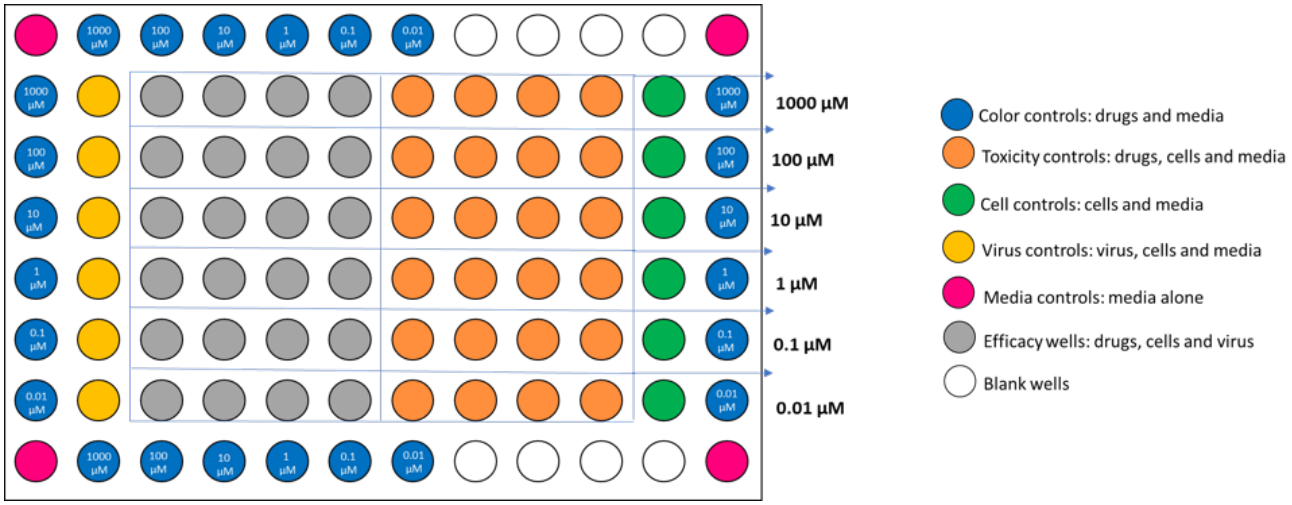

Figure 2-2 Plate layout for testing cytotoxicity and efficacy of ER α-glucosidase inhibitors against Zika virus replication

Controls included color controls with drugs and media, toxicity controls with drugs, cells and media, cell controls with cells and media, virus controls with virus, cells and media, media controls with media alone, efficacy wells with drug, cells and virus and blank wells. ER-AGIs were tested in concentrations ranging from 0.01 µM and 1000 µM.

Adapted from *Fletcher et. al.*

2.6 **Characterizing the effect of ER-AGIs on ZIKV-induced cytopathogenicity**

2.6.1 Caspase-Glo assay

The levels of activated caspase 3 and 7 in Vero and CHME-3 cells was measured using luminescent Promega Caspase-Glo® 3/7 Assay (Promega) following the manufacturer's instructions. Vero and CHME-3 cells seeded in 96-well white-walled cell culture plates (Greiner Bio One, Monroe, NC), were treated with compounds and infected with ZIKV at a MOI of 1 in the same manner as the initial high-throughput antiviral screening plate layout as shown in Figure 2-2. Negative controls were performed without the virus. After 72 hpi, 100 µl of Caspase-Glo® Reagent (Promega) was added to all wells containing cells and reagent blanks with no cells. After incubating the plates at room temperature in the dark for 30 min, a microplate reader was used to record the luminescence. Each sample was read five times and the average was taken (Spark; TECAN) at an interval of 15 sec. Each assay was repeated three times and the data was analyzed using Microsoft Excel and graphed on Prism 7.

2.6.2 Lactate dehydrogenase (LDH) assay

The levels of lactate dehydrogenase in Vero and CHME-3 cells was measured using the CytoTox 96 Non-Radioactive Cytotoxicity Assay (Promega) following the manufacturer's instructions. Vero and CHME-3 cells seeded in 96-well cell culture plates (Denville Scientific Inc.) were treated with compounds and infected with virus at a MOI of 1 in the same manner as the initial antiviral screening as shown in Figure 2-2. Negative controls were performed without the virus. 48 hpi and 72 hpi, 50 µl of supernatant was added to a new 96-well white-walled cell culture plate with the addition of 50 µl of

CytoTox 96® Reagent (Promega) in each well. The plate was incubated in the dark at room temperature for 30 min. After 30 min incubation, 50 µl of Stop Solution (Promega) was added to each well and the optical density was measured at 490 nm using a microplate reader (ELx800; BioTek). Each assay was repeated three times and the data was analyzed using Microsoft Excel and graphed on Prism 7.

2.7 **Investigating the effect of ER-AGIs on ZIKV replication**

ZIKV yield reduction following treatment with the ER α-glucosidase inhibitors was assessed by measuring NS1 gene by relative quantitative reverse transcription PCR (qRT-PCR) assay and infectious virus titration in Vero cells and CHME-3 cells.

2.7.1 Quantification of viral RNA

Vero and CHME-3 cells were infected with PRVABC59 ZIKV either at a MOI of 0.5 or 5 in infection medium. After 2 h of pre-incubation with the virus, medium from cells was removed, cells were washed with PBS and fresh infection medium containing 1 µM of castanospermine, Celgosivir, DNJ or NN-DNJ was added to the wells. At 48 hpi, culture supernatants were harvested and used for measuring virus yield. Three biological replicates were maintained at each time point along with corresponding water or DMSO vehicle controls. Each experiment was repeated three times and the data was analyzed and graphed using Prism 7.

2.7.1.1 Viral RNA extraction and isolation

Viral RNA was extracted using the MagMAX™ Express Viral RNA Isolation kit using a MagMAX™ Express-96 (Applied Biosystems (ABI), Foster City, CA) equipped

with a Deep Well Magnetic Head. According to the manufacturer's protocol, first, 20 µl of Bead Mix was added to the processing plate followed by the addition of 50 µl of sample. Then 130 µl of Lysis/Binding solution was added to the Sample/Bead Mix in the processing plate. In this automated process, paramagnetic beads bound nucleic acids while other contaminants were washed away with Wash Solution 1. The beads were then washed again with Wash Solution 2 to remove any residual binding solution. Finally, nucleic acids were eluted in 50 µl of elution buffer.

2.7.1.2 qRT-PCR analysis

The amount of ZIKV NS1 was measured by qRT-PCR using SuperScript® III One-Step RT-PCR System with Platinum® *Taq* DNA Polymerase on an ABI 7500 Fast machine (ABI) as previously described by Goebel et. al (60). The primers and probes were provided by Integrated Device Technology (IDT, San Jose, CA) and are shown in Table 2-4. The qRT-PCR cycling condition included an initial cDNA synthesis for 30 min at 50 ºC, followed by 2 min at 95 ºC and 45 cycles of 2-step cycling at 95 ºC for 15 s, then 55 ºC for 30 s and this program is shown in Table 2-5. The cell culture supernatant from infected cells was subjected to one-step qRT-PCR assay to detect the ZIKV NS1 gene. The data was measured as relative equivalent units (REU) against a 10-fold dilution series of RNA purified from 10^7 $TCID_{50}$ of ZIKV PRVABC59. A standard curve was plotted using ABI 7500 software and the standard curve was used to calculate the REU viral RNA of test samples. The standard curve is shown in Figure 2-3.

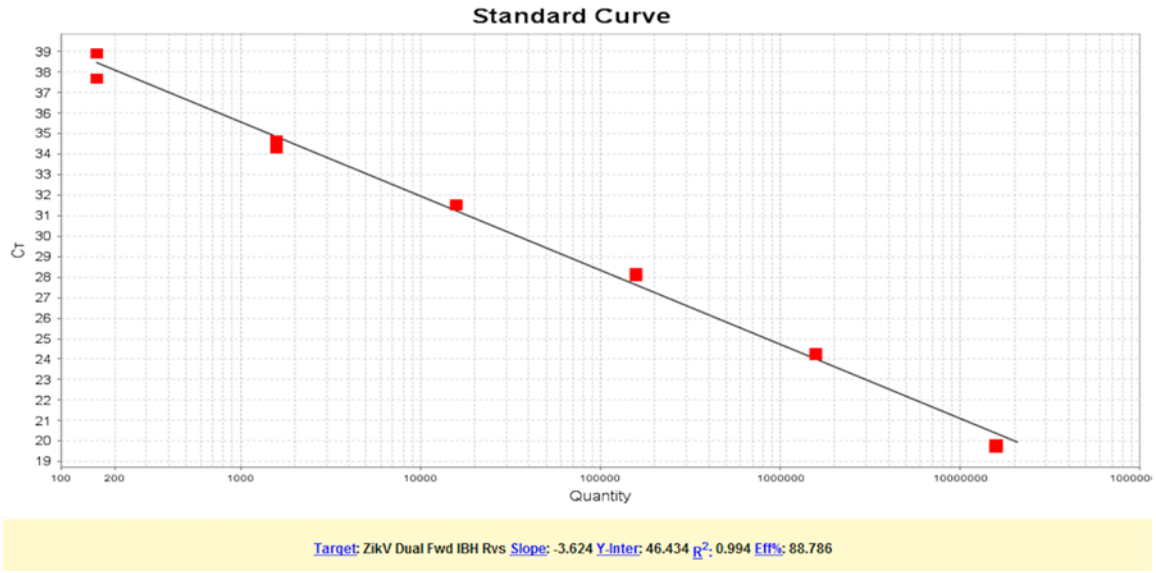

Figure 2-3 Standard curve for the calculation of REU Viral RNA from threshold cycle (Ct) values

Standard curve with slope of -3.624 and efficiency of 88.786% showing linear relation (R^2=0.994) between 10-fold dilution series of RNA purified from 10^7 $TCID_{50}$ of ZIKV PRVABC59 and Ct value of RT-PCR assay, indicating $TCID_{50}$ quantity (values on X axis) can be accurately predicted using average Ct values (values on Y axis)

Table 2-4 Primers for Zika virus gene NS1

Genes	Primer/Probe	Sequence (5'-3')	Reference
IBH 30656 NS1	Forward	ATATCGGACATGGCTTCGGA	(60)
	Reverse	GTTCTTTTACAGACATATTGAGTGTC	
	Probe	FAM −TGCCCAACA/ZEN/CAAGGTGAAGCCTACCT-BHQ	

Table 2-5 Program for *Taq*-based qRT-PCR

Step	cDNA synthesis		Cycle (45 cycles)	
			Denature	Anneal/Extend
Temperature (°C)	50 °C	95 °C	95 °C	55 °C
Time	30 minutes	2 minutes	15 seconds	30 seconds

2.7.2 Infectious virus quantification by $TCID_{50}$

To determine amount of infectious virus, supernatants were titrated using Vero cell infection. Vero cells were seeded in a 96-well plate (Denville Scientific Inc.) and grown to be 100% confluent. Cells were washed with PBS before addition of 146 µl of supernatant in sextuplicate in column 1. This was followed by serially diluting 46 µl of the supernatant across the 96-well plate to create half-log dilutions. Tips were changed after each dilution. Following the final dilution, 46 µl was removed from column 12 and transferred to the waste container. The plate was cultured at 37 °C and was observed for cytopathic effect for 3-4 days. Titer was expressed as $TCID_{50}$/ml calculated using the Reed-Muench method (58).

2.8 **Quantification of antiviral gene response**

Human microglial cells, CHME-3 cells were used to study cellular antiviral gene expression. The cells were grown in 6-well plates and pre-incubated with PRVABC59 at a MOI of 1 for 2 h. After 2 h of pre-incubation with the virus, medium from cells was removed, cells were washed with PBS and fresh infection medium containing 1 µM of Celgosivir was added. The cells were then incubated for 24 h, 48 h and 72 h. Three biological replicates were maintained at each time point along with three corresponding uninfected-untreated controls, three infected-only controls and three compound treated-only controls.

2.8.1 Total RNA extraction

Total RNA was extracted from cells using the RNeasy Plus Minikit (Qiagen, Germantown, MD) according to the manufacturer's protocol. Cells were lysed with RLT buffer with β-mercaptoethanol after complete removal of the media and the lysates were homogenized by QIAshredder (Qiagen) and centrifuged for 2 min at 8000 *g*. The flow-through was transferred to a gDNA eliminator spin column placed in a 2 ml collection tube and centrifuged for 30 s at 8000 *g*. A volume of 70% ethanol was added to the flow-through and mixed well by pipetting. The mixture was then transferred to a RNeasy spin column placed in a 2 ml collection tube and centrifuged for 15 s at 8000 *g*. The flow through was discarded and 500 µl of RPE buffer was added to the RNeasy spin column and centrifuged for 2 min at 8000 *g*. After discarding the flow through, the spin column was placed in a new collection tube and centrifuged for 1 min at 8000 *g*. The spin column was placed in a 1.5 ml Eppendorf tube and 20 µl of RNase-free water was added directly onto the column. Ultimately, to elute RNA, the spin column was centrifuged for 1 min at 8000 *g*. The total RNA concentration was determined by NanoDrop Lite spectrophotometer (Thermo Scientific, Waltham, MA), according to the manufacturer's protocol.

2.8.2 Conversion of total RNA to cDNA

cDNA was synthesized from 1 µg of total RNA using 4 µl of qScript cDNA SuperMix (5x) (QuantaBio, Beverly, MA). qScript cDNA SuperMix contains reaction buffer with $MgCl_2$, dNTPs, ribonuclease inhibitor protein (RIP), qScript reverse transcriptase and titrated concentrations of random hexamer and oligo(dT) primers. Volumes of RNA template and RNase-free water varied depending on each sample's total

RNA concentration with each reaction system subsequently totaling 20 µl. The reaction was incubated at 25 ºC for 5 min, followed by incubation at 42 ºC for 30 min in the Veriti 96-well thermal cycler (ABI). The reaction was terminated by heating at 85 ºC for 5 min and was held at 4 ºC at the end of the run. The program for total RNA to cDNA conversion is shown in Table 2-6. Each synthesized cDNA sample was then diluted 1:25 in RNase/DNase free water for real-time PCR analysis.

Table 2-6 Program for Thermal Cycler PCR reaction for RNA to cDNA conversion

Step				
Temperature (°C)	25 °C	42 °C	85 °C	4 °C
Time	5 minutes	30 minutes	5 minutes	Hold

2.8.3 qPCR analysis of relative gene expression

qPCR was performed based on SYBR chemistry using the ABI 7500 Fast real-time PCR system (ABI). Reaction components and qPCR program are shown in Table 2-7 and 2-8, respectively. For normalization, HPRT1 was chosen as the house-keeping gene. qRT-PCR data was normalized using a relative standard curve method using HPRT1 as a house keeping gene as previously described (61). Serial dilutions of a pooled cDNA sample (combination of virus and mock infected samples and Celgosivir-treated and untreated samples) were used to plot a standard curve. Using the slope of the standard curve, raw Ct values were converted to relative quantities using the equation obtained from the standard curve which are then normalized to HPRT1 values by taking the ratio of treated samples to control samples. Human gene primers are shown in Table 2-9.

2.8.4 House-keeping gene selection

Several house-keeping genes including GAPDH, HMBS, HPRT1 and 18s rRNA were evaluated for their suitability for qPCR normalization in human microglial CHME-3 cell lines infected with ZIKV strain, PRVABC59 and Celgosivir treatment. The least variant gene among these genes tested was found to be HPRT1.

2.9 **Data analysis**

Prism 7 (GraphPad) was used to generate graphs and perform statistical analysis. A one-tailed Welch's T-test was used to compare treated and untreated samples within a group, with α=0.05.

Table 2-7 SYBR-green real-time PCR reaction components

SYBR-green chemistry	
Components	Volume used per reaction (µl)
Nuclease-free water	6.5
Reaction mix	12.5
Forward Primer (10 µM)	0.5
Reverse Primer (10 µM)	0.5
Template cDNA (1:25 dilution)	5
Total volume	25

Table 2-8 Program for SYBR-based qPCR

Step	Hold	Cycle (40 cycles)	
		Denature	Anneal/Extend
Temperature (°C)	95 °C	95 °C	60 °C
Time	10 minutes	15 seconds	60 seconds

Table 2-9 Primers for human genes

Human genes	Primers	Sequence (5'-3')	Reference
Human GAPDH	Forward	GCAAATTTCCATGGCACCGT	(62)
	Reverse	GCCCCACTTGATTTTGGAGG	
Human HMBS	Forward	CTGTTTACCAAGGAGCTGGAAC	(63)
	Reverse	TGAAGCCAGGAGGAAGCA	
Human HPRT1	Forward	GACCAGTCAACAGGGGACAT	(63)
	Reverse	CCTGACCAAGGAAAGCAAAG	
Swine 18s rRNA	Forward	GTAACCCGTTGAACCCCATT	(64)
	Reverse	CCATCCAATCGGTAGTAGCG	
Human IFNβ	Forward	ACCTCCGAAACTGAAGATCTCCTA	(65)
	Reverse	TGCTGGTTGAAGAATGCTTGA	
Human IRF7	Forward	CCCCATCTTCGACTTCAGAG	(66)
	Reverse	AAGGAAGCACTCGATGTCGT	
Human RIG-I	Forward	GCCATTACACTGTGCTTGGAGA	(67)
	Reverse	CCAGTTGCAATATCCTCCACCA	
Human MDA5	Forward	GGCACCATGGGAAGTGATT	(68)
	Reverse	TTTGGTAAGGCCTGAGCTG	
Human MX-1	Forward	CCAGCTGCTGCATCCCACCC	(69)
	Reverse	AGGGGCGCACCTTCTCCTCA	
Human ISG15	Forward	AGCTGAAGGCGCAGATCACCC	(70)
	Reverse	GCGCAGATTCATGAACACGGTGC	

Chapter 3
Results

3.1 Evaluation of ER-AGI cytotoxicity in Vero cells or CHME-3 cells

A total of four iminosugars namely, castanospermine, Celgosivir, DNJ and NN-DNJ were tested for cytotoxicity in Vero and CHME-3 cells at concentrations ranging from 0.01 μM to 1000 μM by a previously described high-throughput drug screening assay (59). Cytotoxicity of the compounds was first explored to ensure that no cytotoxicity was induced in either cell line. If cytotoxicity was seen at low concentrations, we would not be able to proceed with further studies looking into ER-AGI efficacy against ZIKV infection. Secondly, the cytotoxicity screen was used to determine the range of concentrations to use for further efficacy studies. There was no reduction in absorbance in compound-treated cells in comparison to vehicle controls. No decrease in cell viability in iminosugar-treated cells in comparison to vehicle-treated cells showed that castanospermine, Celgosivir, DNJ and NN-DNJ did not induce cytotoxicity in Vero (Fig. 3-1A) or CHME-3 cells (Fig. 3-1B) at concentrations ranging from 0.01 μM to 100 μM. At 1000 μM concentrations of castanospermine, Celgosivir and DNJ, absorbance levels were below water vehicle-treated cells indicating that there was some cytotoxicity. However, more severe cytotoxicity was noted at 1000 μM of NN-DNJ in both Vero and CHME-3 cells as evidenced by a notably low absorbance value in comparison to vehicle treated samples.

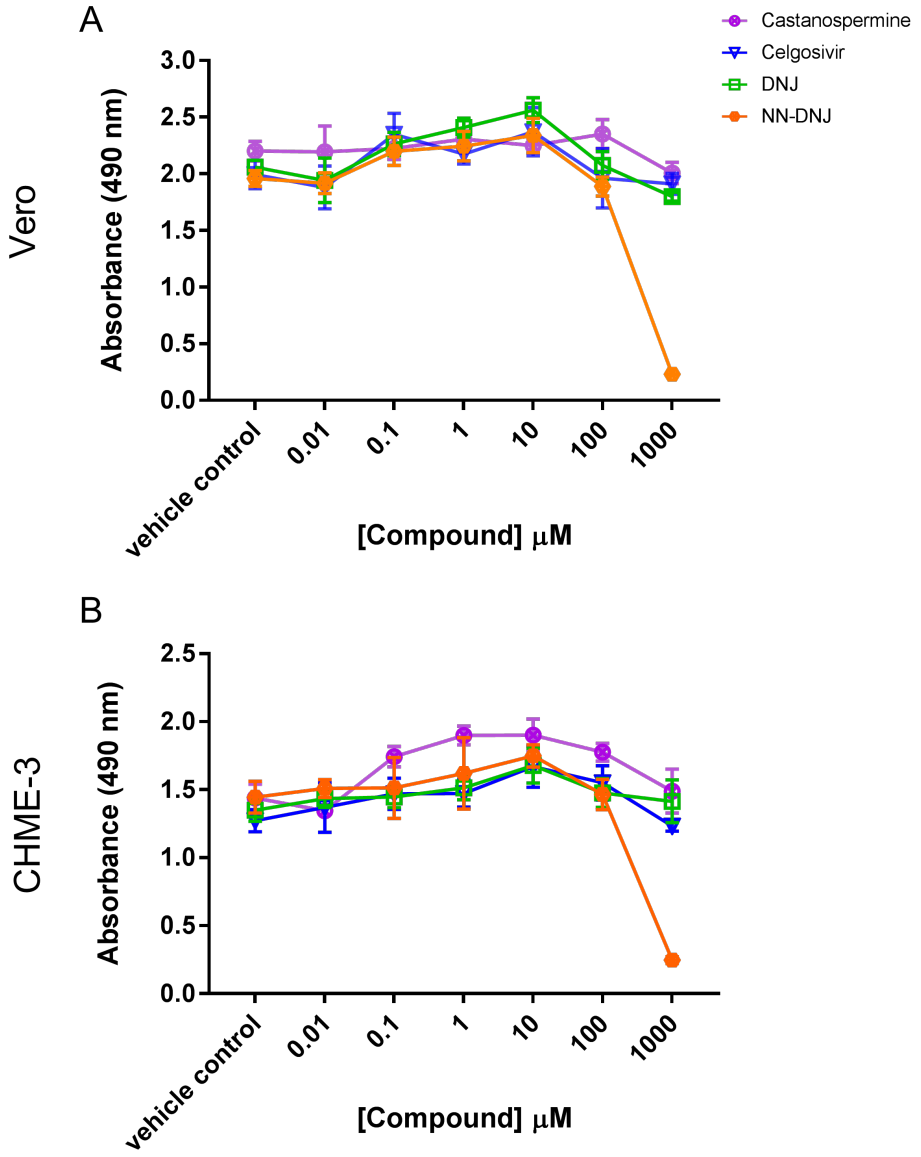

Figure 3-1 Cytotoxicity of iminosugars in Vero cells and CHME-3 cells

A) Cytotoxicity in Vero cells and **B)** CHME-3 cells. Cells were treated with castanospermine, Celgosivir, DNJ and NN-DNJ in concentrations ranging from 0.01 μM to 1000 μM and quantified by MTS assay at 72 hours post treatment. No cytotoxicity was found in cells treated with compounds in concentrations ranging from 0.01 μM to 100 μM in comparison to vehicle controls. Moderate toxicity was seen in cells treated with 1000 μM of castanospermine, Celgosivir and DNJ. More severe cytotoxicity was seen in cells treated with 1000 μM of NN-DNJ. Absorbance was measured at 490 nm. Data represents mean absorbance of four biological replicates. Error bar = SD

3.2 **Effects of ER-AGI treatment on virus replication**

To evaluate the ability of ER-AGIs to inhibit ZIKV replication, we compared viral RNA and infectious virus in culture supernatants of PRVABC59 infected Vero and CHME-3 cells at 48 hpi. Based off previous research we would expect to see a reduction in viral RNA and infectious virus titers upon the addition of ER-AGIs due to the fact that ER-AGIs are blocking the proper folding and maturation of viral glycoproteins which contain functions critical to ZIKV replication cycle. Significant reduction ($p<0.05$) ZIKV RNA were seen in supernatants of Vero cells treated with 1 μM of castanospermine (Fig. 3-2A), Celgosivir (Fig. 3-3A) and DNJ (Fig. 3-4A) in comparison to vehicle controls. Similar reductions in viral RNA were seen between cells infected at a MOI of 0.5 as well as a MOI of 5. While a similar significant reduction of viral RNA was also observed in CHME-3 cells infected at MOI of 0.5 (Fig. 3-2C, 3-3C, and 3-4C), the reduction in viral RNA was not significant between castanospermine treated and control cells infected at MOI of 5.0 (Fig. 3-2C).

Upon quantification of infectious ZIKV particles by $TCID_{50}$ method, castanospermine, Celgosivir and DNJ were able to reduce infectious ZIKV particles by a half-log to log in both Vero and CHME-3 cells in comparison to vehicle controls (Fig. 3-2B and D, 3-3B and D, 3-4B and D). The reduction in infectious virus particles was not significant between castanospermine-treated CHME-3 cells and control cells infected at MOI of 0.5 (3-2D). No significant reductions in viral RNA and infectious virus particles was seen in Vero cells treated with NN-DNJ (3-5A and 3-5B). In CHME-3 cells with NN-

DNJ treatment, a significant reduction of viral RNA (3-5C) but not infectious virus particles (3-5D) was observed.

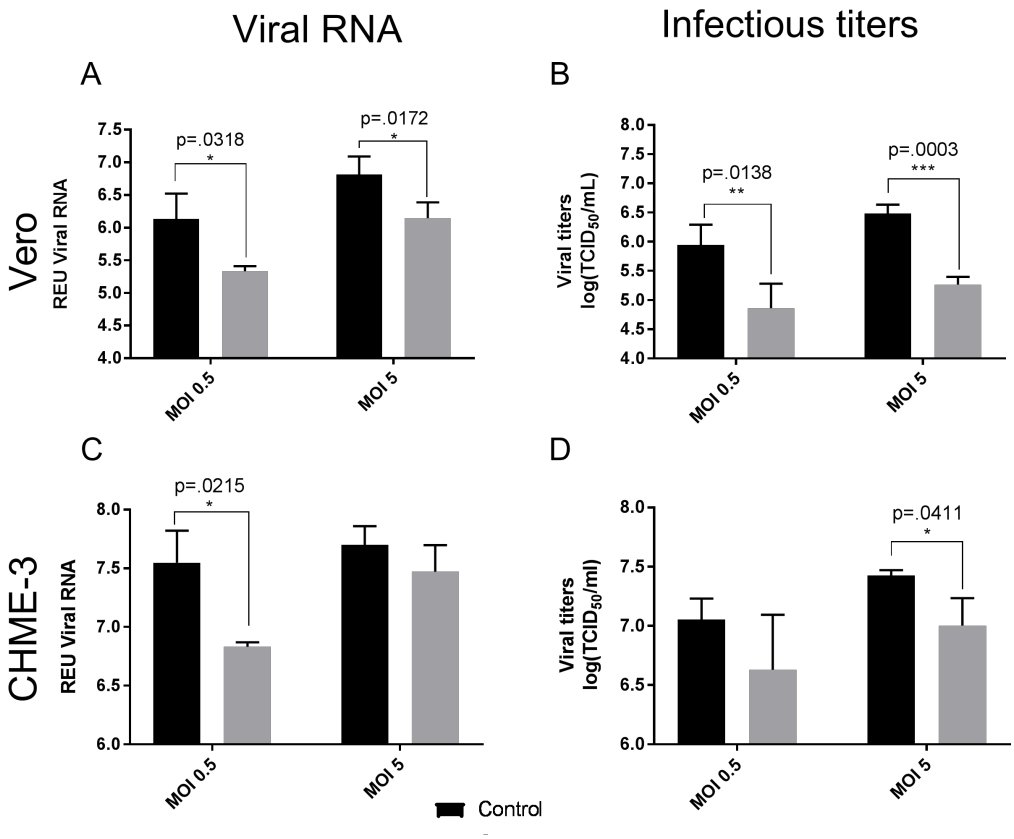

Figure 3-2 Quantification of ZIKV NS1 gene and infectious virus titers in cell culture supernatants of Vero and CHME-3 cells after PRVABC59 infection and Castanospermine treatment.

A) Vero cells and **C)** CHME-3 cells infected with PRVABC59 at MOI of 0.5 or 5 with and without 1 μM castanospermine treatment were harvested at 48 hpi and relative equivalent units (REU) viral RNA levels were determined by real-time PCR quantitation of ZIKV NS1 gene in culture supernatants of African green monkey kidney Vero cells and human microglial CHME-3 cells. Data are representative of one of three independent experiments and values are expressed as means of three biological replicates. Error bar = SD.

Infectious ZIKV titration in supernatant of **B)** Vero cells and **D)** CHME-3 cells infected with PRVABC59 at MOI of 0.5 or 5 with or without 1 μM castanospermine treatment at 48 hpi was determined by $TCID_{50}$ assay method. Data shown were means of three biological replicates, Error bar = SD * $p< 0.05$, ** $p<0.01$, *** $p<0.001$

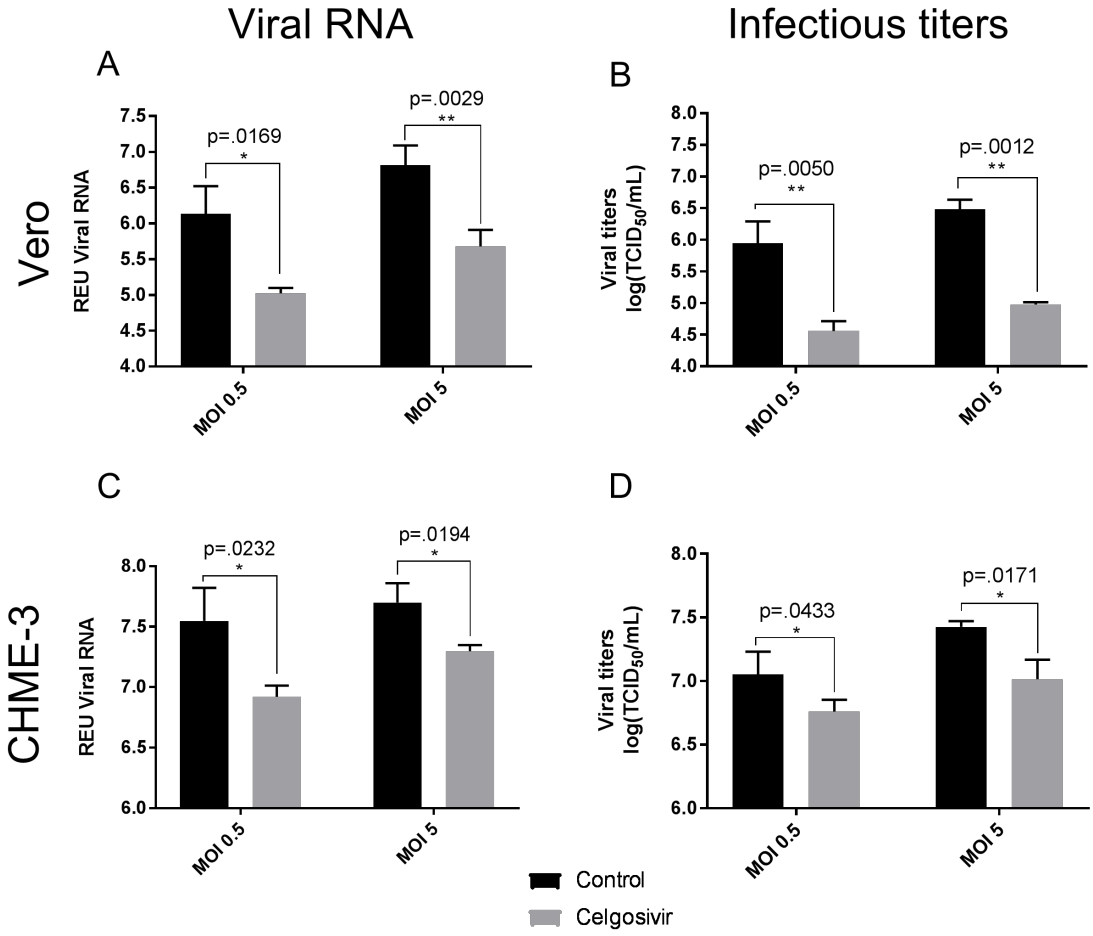

Figure 3-3 Quantification of ZIKV NS1 gene and infectious virus titers in cell culture supernatants of Vero and CHME-3 cells after PRVABC59 infection and Celgosivir treatment.

A) Vero cells and **C)** CHME-3 cells infected with PRVABC59 at MOI of 0.5 or 5 with and without 1 µM Celgosivir treatment were harvested at 48 hpi and relative equivalent units (REU) viral RNA levels were determined by real-time PCR quantitation of ZIKV NS1 gene in culture supernatants of African green monkey kidney Vero cells and human microglial CHME-3 cells. Data are representative of one of three independent experiments and values are expressed as means of three biological replicates. Error bar = SD.

Infectious ZIKV titration in supernatant of **B)** Vero cells and **D)** CHME-3 cells infected with PRVABC59 at MOI of 0.5 or 5 with or without 1 µM Celgosivir treatment at 48 hpi was determined by $TCID_{50}$ assay method. Data shown were means of three biological replicates, Error bar = SD * $p< 0.05$, ** $p<0.01$, *** $p<0.001$

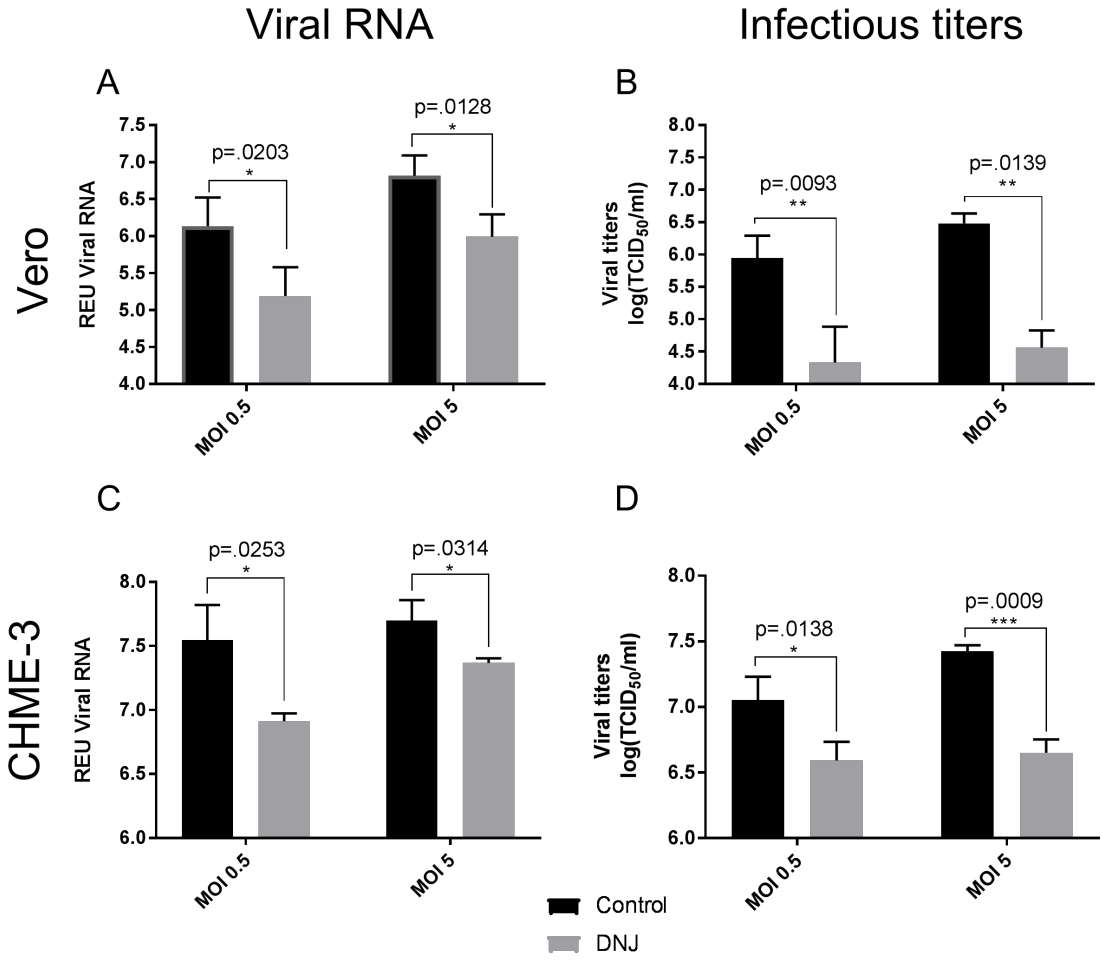

Figure 3-4 Quantification of ZIKV NS1 gene and infectious virus titers in cell culture supernatants of Vero and CHME-3 cells after PRVABC59 infection and Deoxynojirimycin (DNJ) treatment.

A) Vero cells and **C)** CHME-3 cells infected with PRVABC59 at MOI of 0.5 or 5 with and without 1 μM DNJ treatment were harvested at 48 hpi and relative equivalent units (REU) viral RNA levels were determined by real-time PCR quantitation of ZIKV NS1 gene in culture supernatants of African green monkey kidney Vero cells and human microglial CHME-3 cells. Data are representative of one of three independent experiments and values are expressed as means of three biological replicates. Error bar = SD.

Infectious ZIKV titration in supernatant of **B)** Vero cells and **D)** CHME-3 cells infected with PRVABC59 at MOI of 0.5 or 5 with or without 1 μM DNJ treatment at 48 hpi was determined by $TCID_{50}$ assay method. Data shown were means of three biological replicates, Error bar = SD * $p< 0.05$, ** $p<0.01$, *** $p<0.001$

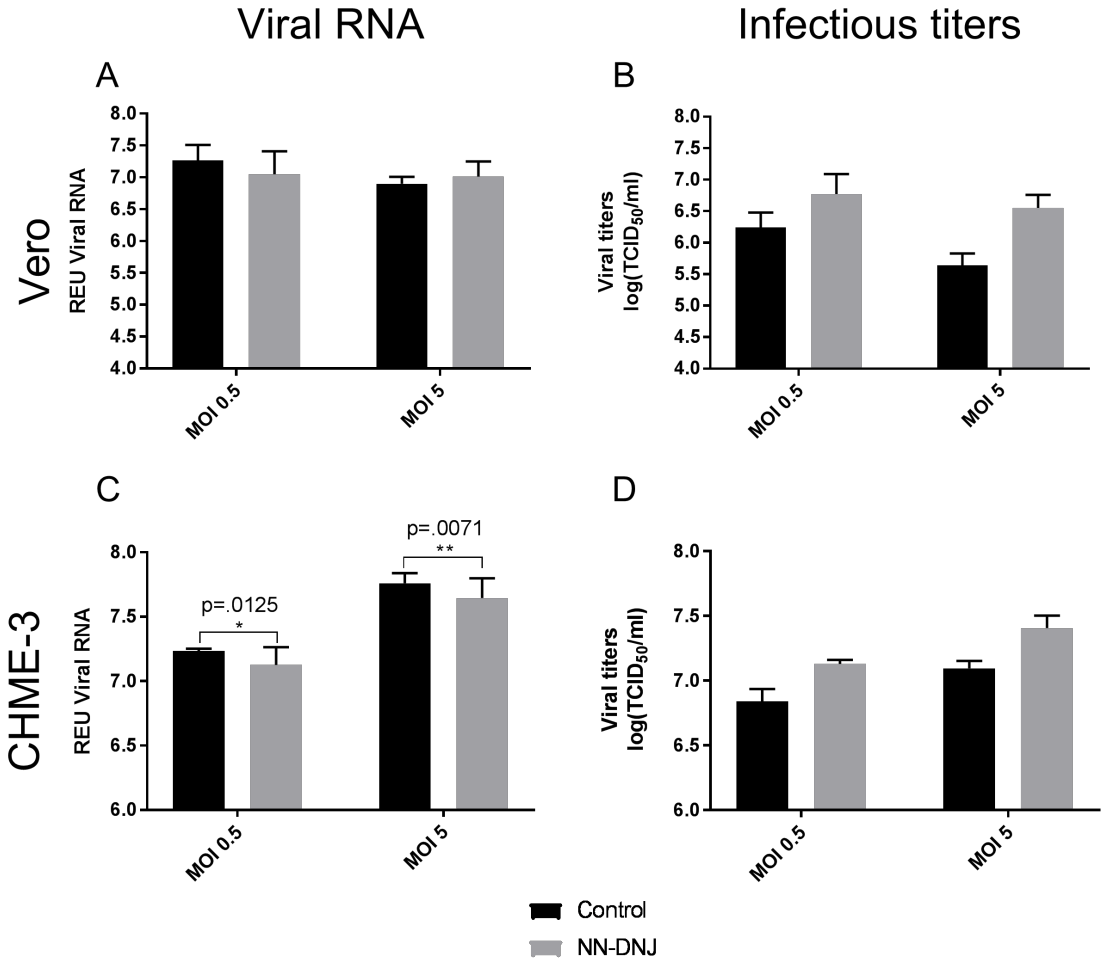

Figure 3-5 Quantification of ZIKV NS1 gene and infectious virus titers in cell culture supernatants of Vero and CHME-3 cells after PRVABC59 infection and N-Nonyl Deoxynojirimycin (NN-DNJ) treatment.

A) Vero cells and **C)** CHME-3 cells infected with PRVABC59 at MOI of 0.5 or 5 with and without 1 μM NN-DNJ treatment were harvested at 48 hpi and relative equivalent units (REU) viral RNA levels were determined by real-time PCR quantitation of ZIKV NS1 gene in culture supernatants of African green monkey kidney Vero cells and human microglial CHME-3 cells. Data are representative of one of three independent experiments and values are expressed as means of three biological replicates. Error bar = SD.

Infectious ZIKV titration in supernatant of **B)** Vero cells and **D)** CHME-3 cells infected with PRVABC59 at MOI of 0.5 or 5 with or without 1 μM NN-DNJ treatment at 48 hpi was determined by $TCID_{50}$ assay method. Data shown were means of three biological replicates, Error bar = SD * $p< 0.05$, ** $p<0.01$, *** $p<0.001$

3.3 **Regulation of human cell antiviral gene expression upon ZIKV infection**

Virus infection of most cells results in an upregulation of antiviral gene expression. Hence, we first investigated the effect of ZIKV infection on the antiviral gene response in human microglial cells, CHME-3 cells were infected with PRVABC59 at MOI of 1 and expression levels of antiviral genes namely MDA5, RIGI, MX1, IRF7, IFNβ and ISG15 were quantified by qPCR in virus and mock infected cells at 24, 48 and 72 hpi. All of the genes were significantly upregulated ($p<0.05$) at 48 and 72 hpi. No significant difference was observed between virus and mock infected cells at 24 hpi. The difference between PRVABC59-infected and mock-infected cells was most clear with IFNβ at 72 hpi (Fig. 3-6E), RIGI at 48 hpi (Fig. 3-6B) and MX1 at 72 hpi (Fig. 3-6C). Of all the genes studied only RIGI was reduced in both PRVABC559 and mock-infected at 72 hpi (Fig. 3-6C).

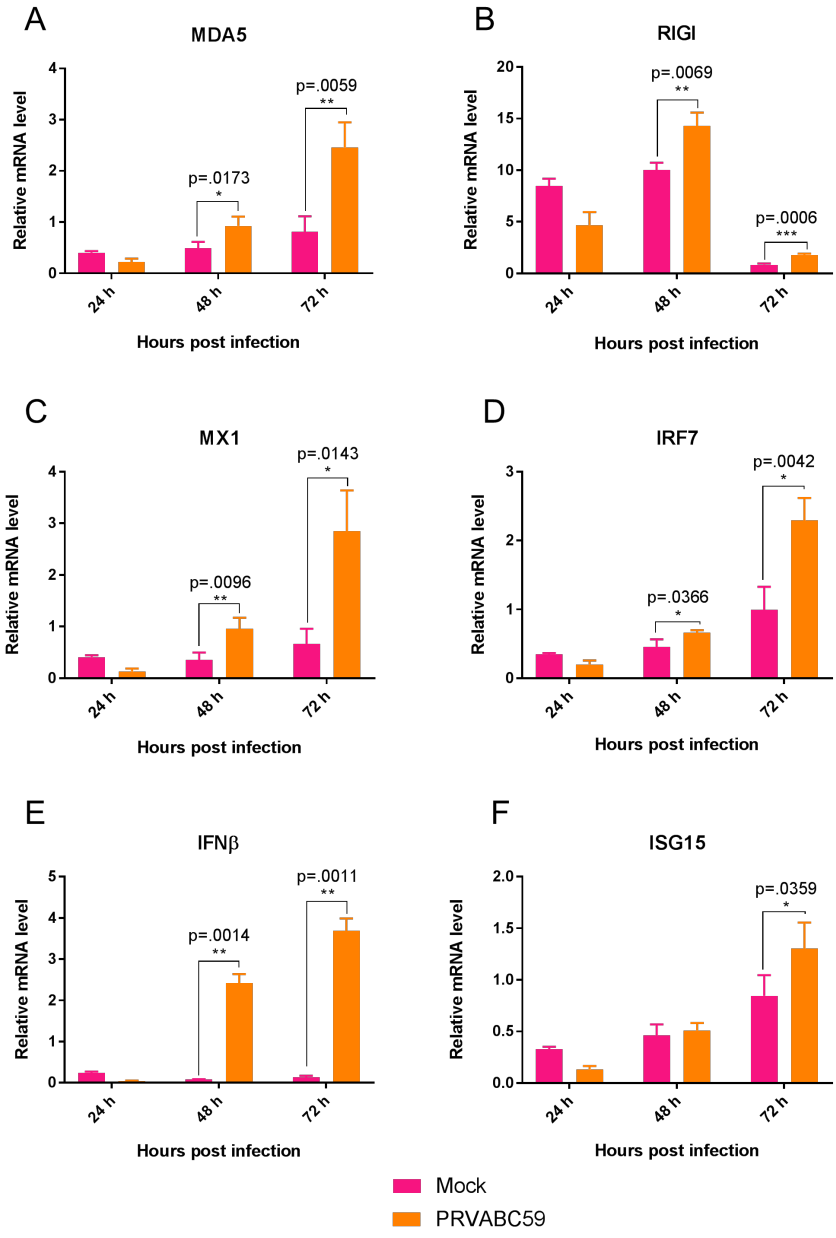

Figure 3-6 Human CHME-3 cell antiviral gene expression profiles upon PRVABC59 infection.

Relative mRNA expression profiles of **A)** MDA5, **B)** RIGI, **C)** MX1, **D)** IRF7, **E)** IFN, **F)** ISG15 at 24 hpi, 48 hpi and 72 hpi. Antiviral gene levels are increased in comparison to mock samples, most notably at 72 hours post infection, with the exception of RIGI. This data is derived from triplicate RNA samples and the data points are the ratio between ZIKV-infected to mock-infected samples normalized to HPRT1 gene expression with error bars showing standard deviation. * $p< 0.05$, ** $p<0.01$, *** $p<0.001$

3.4 **Effects of ER-AGIs on human cell antiviral gene expression following ZIKV infection**

Several phytochemicals and other antiviral compounds have been known to cause immunomodulatory as well as antiviral effects *in vitro*. For example, resveratrol potently inhibited both NF-κB activation and NF-κB-dependent gene expression (71, 72). ER-AGIs are known to reduce virus replication by inhibiting viral glycoprotein maturation and not by altering the cellular antiviral response. To further ensure that the immune gene regulation of ER-AGI-treated cells was not altered, the effect of ER-AGIs on infected and uninfected CHME-3 cells was observed. If ER-AGIs were in fact altering the cellular antiviral response, we would expect to see a difference in relative mRNA expression of key antiviral genes in cells that were treated with ER-AGIs in comparison to those that were not. Untreated PRVABC59-infected CHME-3 cells were compared to Celgosivir-treated, PRVABC59-infected cells and no difference was found in relative mRNA levels between the two groups (Fig. 3-7). As seen previously in Figure 3-6, mRNA levels of antiviral genes increased from 24 hpi to 72 hpi in both groups in response to ZIKV infection. As shown in Figure 3-6B, RIGI did not follow this trend and had decreased relative mRNA levels at 72 hpi (Fig. 3-7B) as seen in Fig. 3-6B. The effect of ER-AGIs on uninfected CHME-3 cells treated with and without 1 μM of Celgosivir was investigated (Fig. 3-8). Following previous trends, ER-AGIs do not have an effect on human antiviral

gene expression, even at basal levels. Relative mRNA levels were low due to the fact that cells were not infected with Zika virus.

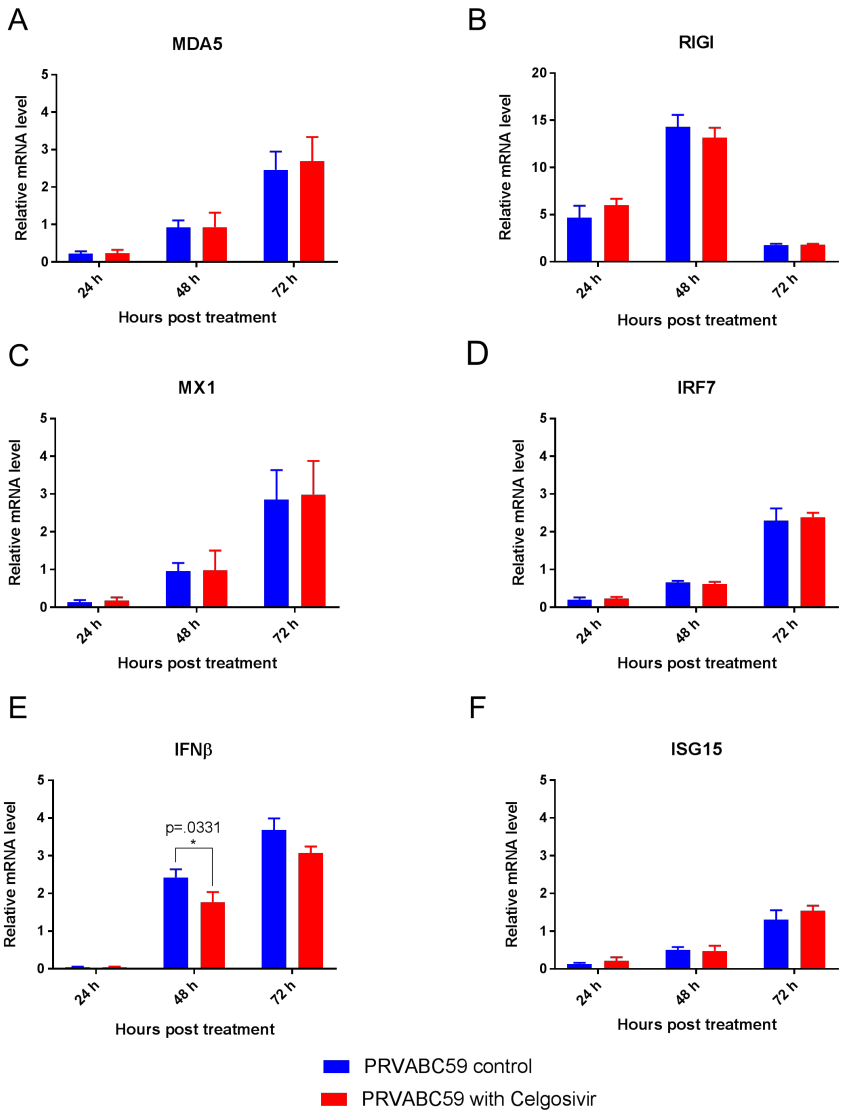

Figure 3-7 Human CHME-3 cell antiviral gene expression profiles following PRVABC59 and Celgosivir treatment.

Relative mRNA expression profiles of **A)** MDA5, **B)** RIGI, **C)** MX1 **D)** IRF7, **E)** IFNβ and **F)** ISG15 at 24 hpt, 48 hpt and 72 hpt. Cellular antiviral gene levels did not differ between PRVABC59-infected Celgosivir-untreated or treated samples. This data is derived from triplicate RNA samples and the data points are the ratio between ZIKV-infected and Celgosivir treated samples to ZIKV-infected untreated samples normalized to HPRT1 gene expression with error bars showing standard deviation. * $p< 0.05$, ** $p<0.01$, *** $p<0.001$

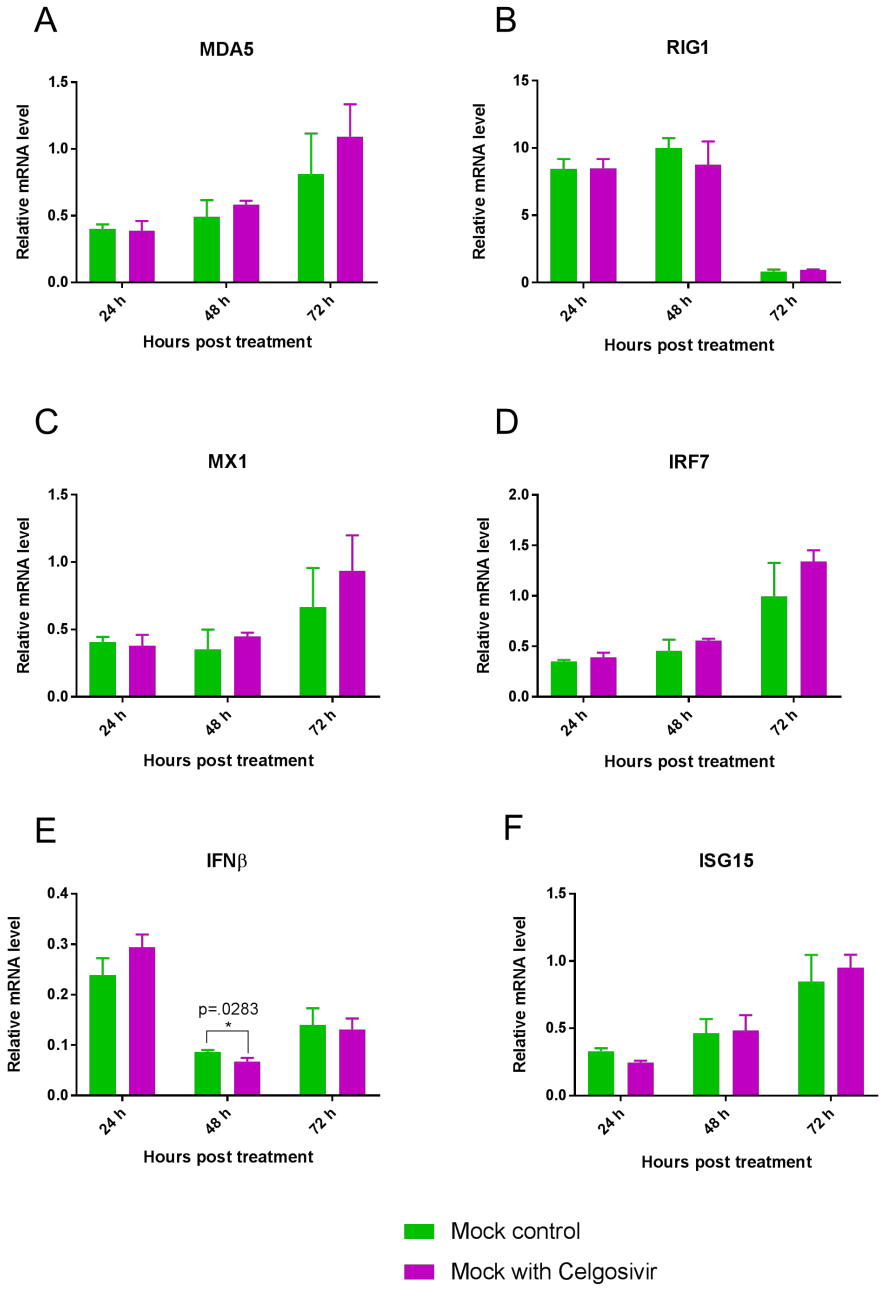

Figure 3-8 Human CHME-3 cell antiviral gene expression profiles following Celgosivir treatment.

Relative mRNA expression profiles of **A)** MDA5, **B)** RIGI, **C)** MX1, **D)** IRF7, **E)** IFN and **F)** ISG15 at 24 hpt, 48 hpt and 72 hpt. Cellular antiviral gene levels did not differ between Celgosivir-untreated or treated samples. This data is derived from triplicate RNA samples and the data points are the ratio between Celgosivir-treated samples to untreated control samples normalized to HPRT1 gene expression with error bars showing standard deviation. * $p < 0.05$, ** $p<0.01$, *** $p<0.001$

3.5 **ER-AGI treated cells show significantly less cytopathogenicity following ZIKV infection**

Iminosugars were further evaluated for ER-AGI activity against three ZIKV isolates in Vero cells, 1) PRVABC59, an Asian strain isolated from a human patient in Puerto Rico in 2015, 2) IBH30656, an African strain isolated from a human patient in Nigeria in 1968 and 3) MEX 2-81, an Asian strain isolated from an *Aedes aegypti* mosquito in Mexico in 2016. ZIKV replication induces cytopathic effect which can be examined under the microscope. Since it was established that ER-AGIs decreased virus replication in section 3.2, we subsequently wanted to see if the cytopathic effect was also decreased.

All four ER-AGIs were similar in their ability to reduce cell death induced by all three ZIKV strains. Vero cells infected with PRVABC59, IBH30656 or MEX 2-81 showed 50-55% cell death at 72 hpi. ER-AGIs ranging from 0.01 μM to 1000 μM were able to rescue the extent of cell death by 30-40% (Fig. 3-9A-D). These isolates represent strains isolated from 1968 to 2016 from different geographic locations, time periods, hosts and lineages, and results show that ER-AGIs similarly inhibit cell death induced by all three isolates.

ER-AGI activity was further assessed against PRVABC59 in CHME-3 cells (Fig. 3-10). 1-10 μM of each compound was the most effective in reducing ZIKV-induced cell death. Generally, PRVABC59-infected CHME-3 cells alone underwent 21-45% cell death. ER-AGIs were able to rescue the quantity of viable cells by approximately 40% as compared to untreated PRVABC59-infected CHME-3. DNJ was most efficacious in reducing PRVABC59-induced cell death in CHME-3 cells. DNJ in concentrations ranging

from 0.01 μM to 100 μM resulted in complete reduction of cell death at 72 hpi compared to untreated PRVABC59-infected CHME-3 cells (Fig. 3-10).

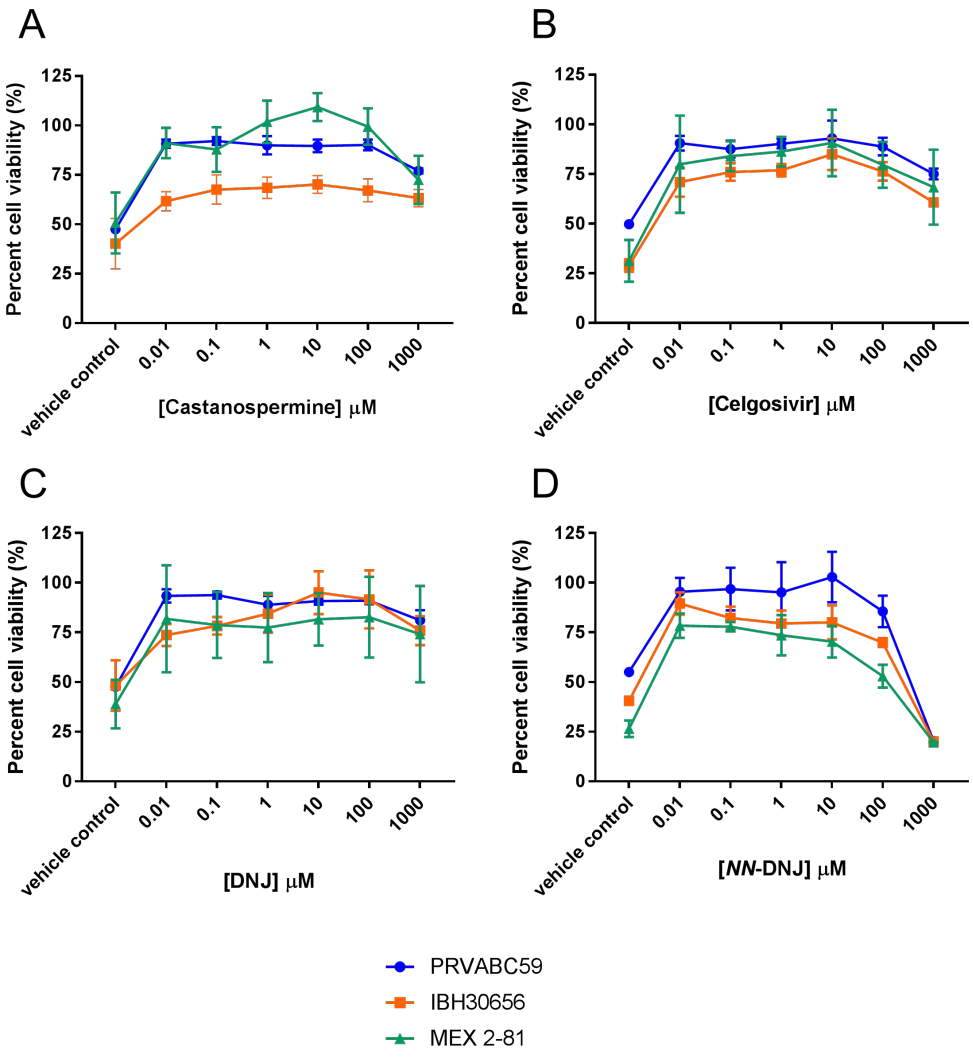

Figure 3-9 Cell viability of ZIKV strain-infected Vero cells with iminosugar treatment

Vero cell viability of **A)** castanospermine **B)** Celgosivir **C)** DNJ and **D)** NN-DNJ-treated or untreated cells infected with ZIKV strain PRVABC59, IBH30656 and MEX 2-81 measured by MTS assay at 72 hpi. ER-AGIs were similar in their ability to effectively rescue cell viability of Vero cells infected with either PRVABC59, IBH306556 or MEX 2-81. Uninfected vehicle controls were set at 100% viability. Absorbance was measured at 490 nm. Data represents mean percent viability of four biological replicates.

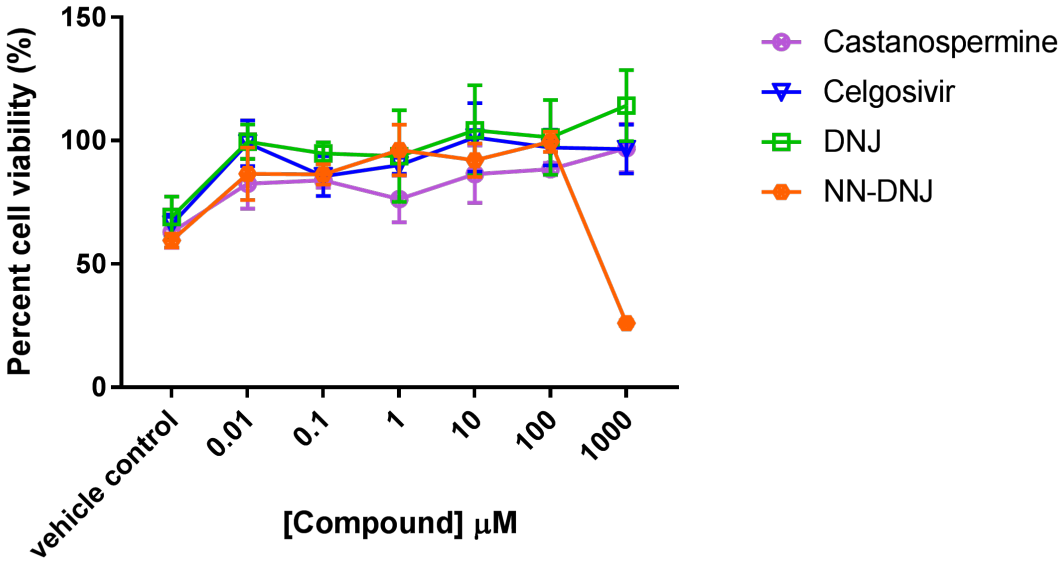

Figure 3-10 Cell Viability of PRVABC59-infected CHME-3 cells with iminosugar treatment.

CHME-3 cell viability of castanospermine, Celgosivir, DNJ and NN-DNJ-treated or untreated cells infected with ZIKV strain PRVABC59, measured by MTS assay at 72 hpi. ER-AGIs were similar in their ability to effectively rescue cell viability of CHME-3 cells infected with PRVABC59. 1000 μM of NN-DNJ did not rescue ZIKV-infected CHME-3 cells. Uninfected vehicle controls were set at 100% viability. Absorbance was measured at 490 nm. Data represents mean percent viability of four biological replicates.

3.6 **ER-AGIs do not alter levels of activated caspase 3/7**

ZIKV has been shown to induce apoptosis in different sets of cells, such as fetal neural progenitor cells (NPC), Cranial Neuro Crest cells, peripheral neurons, dendritic cells and microglia (73-79). The association between ZIKV infection and neuropathologies in humans is well established. To understand the underlying effects of ER-AGIs on ZIKV cytopathogenicity, an activated caspase 3/7 assay was used to study apoptosis, programmed cell death. CHME-3 infection with strain PRVABC59 at MOI 1 substantially increased activated caspase 3 and caspase 7 levels at 48 and 72 hpi. Celgosivir and DNJ were chosen as the representative ER-AGIs of the bicyclic and monocyclic iminosugar groups, respectively. Both ER-AGIs did not significantly reduce levels of activated caspase 3/7 in comparison to untreated CHME-3 cells infected with PRVABC59 at both 48 hpi and 72 hpi (Fig. 3-11A and B and 3-11C and D). At both 48 hpi and 72 hpi, 1000 μM of Celgosivir and DNJ slightly decreased activated caspase 3/7 levels but not significantly ($p > 0.05$).

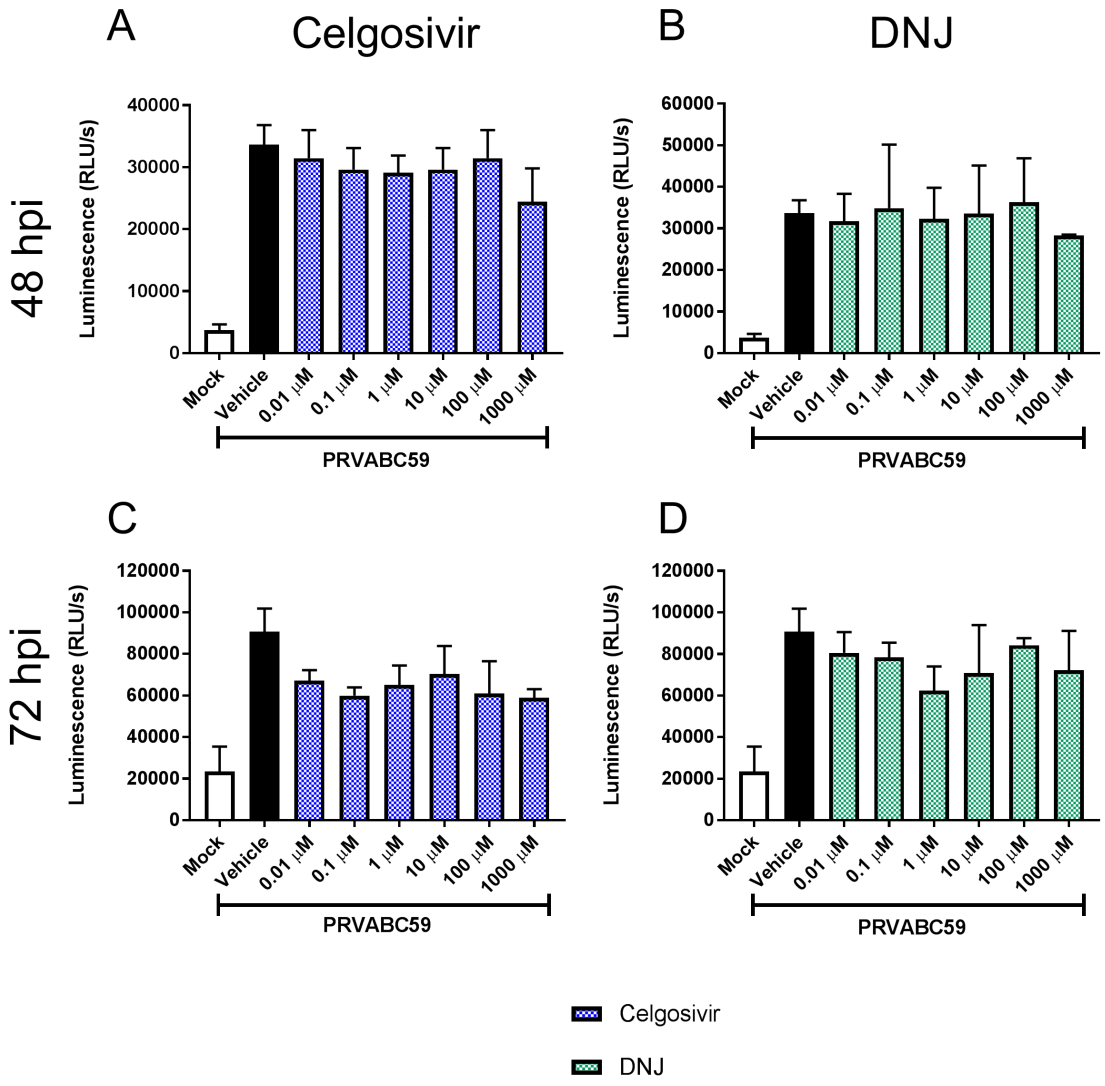

Figure 3-11 Measurement of activated caspase 3/7 in CHME-3 cells following PRVABC59 infection and ER-AGI treatment.

ER-AGIs in concentrations ranging from 0.01 μM to 1000 μM did not reduce activated caspase 3/7 levels after PRVABC59 infection at a MOI of 1 at 48 or 72 hours post infection. Luminescence of CHME-3 cells treated with **A)** Celgosivir 48 hpi, **B)** DNJ 48 hpi, **C)** Celgosivir 72 hpi and **D)** DNJ 72 hpi. Luminescence of each sample was measured using a microplate luminometer. Data represents mean luminescence of four biological replicates with error bars showing standard deviation.

3.7 **ER-AGIs reduce lactate dehydrogenase levels 72 hours post infection**

ZIKV has been shown to cause necrosis in human brain microvascular endothelial cells (HMBECs), especially at 48, 72 and 96 hpi (80). Additionally, histopathological changes such as necrosis have been seen in congenitally ZIKV-infected newborn brains (81). Therefore, the effect of ER-AGIs on cytopathogenicity was further characterized by a lactate dehydrogenase (LDH) activity assay to detect necrosis. CHME-3 cells were infected at a MOI of 1 with PRVABC59 and treated with either 1 μM of Celgosivir and DNJ. CHME-3 infection with strain PRVABC59 alone substantially increased LDH levels at 48 and 72 hpi. 48 h post infection both ER-AGIs tested did not reduce levels of LDH at any observed concentration (Fig. 3-12A and B). However, at 72 hpi DNJ reduced LDH levels by 0.1 absorbance units (Fig. 3-12D) and Celgosivir reduced LDH activity by 0.15 absorbance units (Fig. 3-12C) in comparison to untreated CHME-3 cells infected with PRVABC59. Celgosivir treatment at 72 hpi significantly reduced LDH levels at all concentrations tested (3-12C). DNJ significantly reduced LDH at 72 hpi at 100 and 1000 μM concentrations ($p < 0.05$) (Fig. 3-12D).

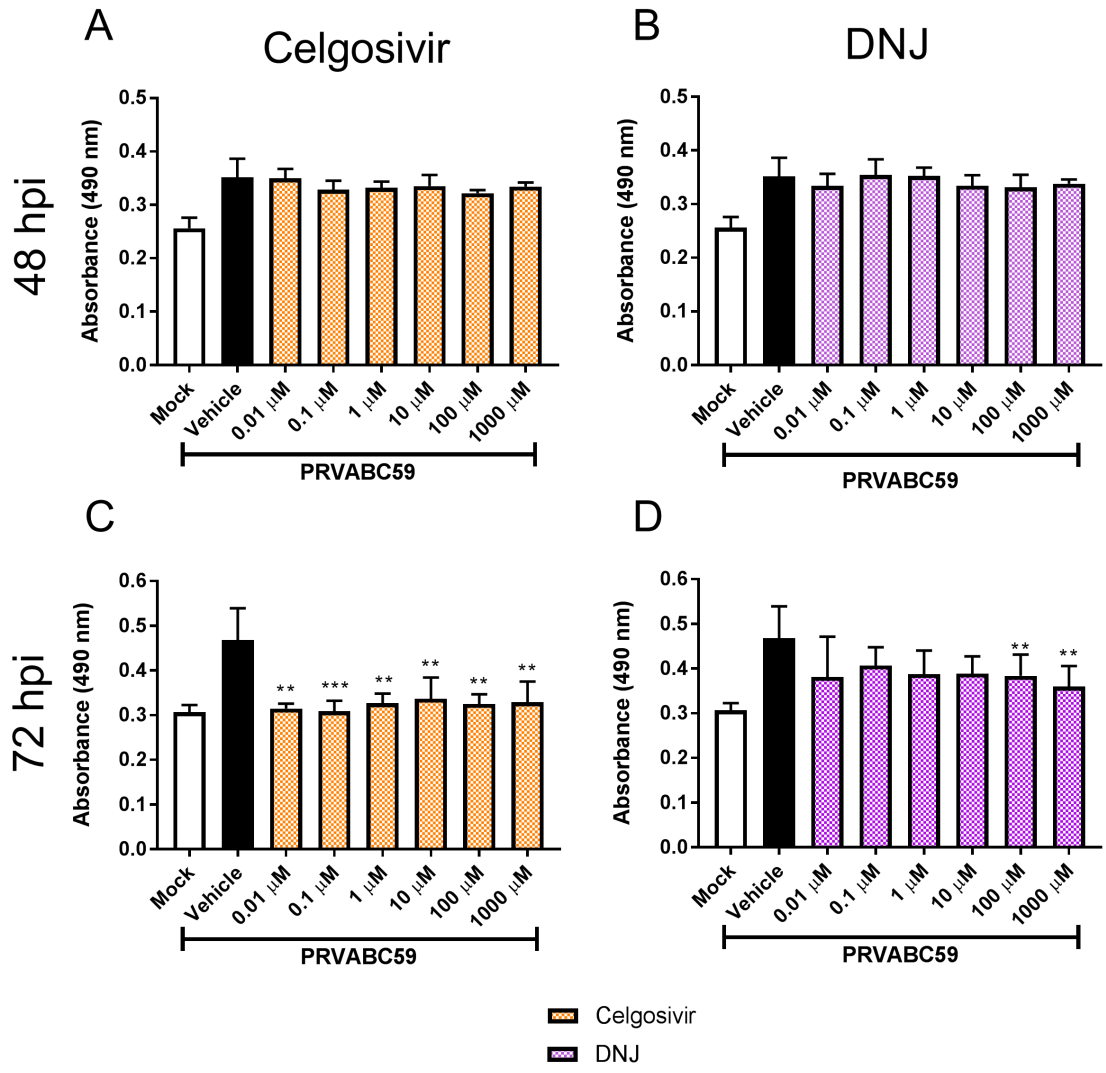

Figure 3-12 Measurement of lactate dehydrogenase in CHME-3 cells following PRVABC59 infection and ER-AGI treatment.

ER-AGIs in concentrations ranging from 0.01 μM to 1000 μM did not reduce activated LDH levels after PRVABC59 infection at a MOI of 1 at **A)** and **C)** 48 hpi. However, at **B)** 72 hpi Celgosivir showed a higher reduction in LDH levels than **D)** DNJ after PRVABC59 infection. Absorbance was measured at 490 nm. Data represents mean absorbance of four biological replicates with error bars showing standard deviation. * $p < 0.05$, ** $p<0.01$, *** $p<0.001$

Chapter 4
Discussion and Conclusions

Although Zika virus (ZIKV) continues to spread throughout the world and continues to be a major health concern worldwide, no specific interventions are currently available except for supportive care such as antipyretics and analgesics. No vaccines or antivirals to prevent devastating neurological syndromes such as meningoencephalitis and microcephaly exist (9). Hence, there is an urgent need to investigate and evaluate novel antiviral therapies for ZIKV infection. In this study, we selected four iminosugars with ER α-glucosidase inhibitor (ER-AGI) activity with different chemical structures to investigate their ability to inhibit ZIKV replication in Vero and human microglial CHME-3 cells.

The results of this study are consistent with other published data showing the potential of ER-AGIs as potent antivirals not only against flaviviruses but other enveloped viruses such as HIV, EBOV, MARV, IAV, HBV, HCV, JEV, WNV, DENV, BVDV, VSV, CMV, Sindbis virus, HSV and ZIKV (50, 52, 55-57, 82-88). Flaviviruses are extremely reliant on ER alpha-glucosidases I and II for N-linked oligosaccharide trimming of their glycoproteins which allow for subsequent interactions with ER chaperones calnexin and calreticulin. ER alpha-glucosidase I removes the terminal α(1,2)-linked glucose from $Glc_3Man_9GlcNAc_2$, and α-glucosidase II removes the second and third glucose before further processing to become a mature virion (89). These enzymes were shown to be important for virus replication when ER alpha-glucosidases I and II knockouts were generated in Huh7.5 cells. ER alpha-glucosidases I and II knockouts had significantly less virus replication of DENV, YFV and ZIKV in comparison to wildtype Huh 7.5 cells which

further confirm ER alpha-glucosidases I and II enzymes as antiviral targets for these three flaviviruses (52).

We observed that three out of four iminosugars inhibit virus replication in both Vero and CHME-3 cells when infected at a MOI of 0.5 and 5 (Fig. 3-2, 3-3 and 3-4). This is in concordance with other studies that showed that ER-AGIs inhibit replication of several enveloped viruses such as hepatitis C virus, dengue virus (DENV), human immunodeficiency virus (HIV), influenza A virus, cytomegalovirus and bovine viral diarrhea virus (51).

Preliminary research of ER-AGIs on ZIKV infection have shown that IHVR-19029, a leading iminosugar inhibited ZIKV replication shown by a decrease in ZIKV RNA in comparison to untreated cells. The EC_{50} of IHVR-19029 was 30 μM in ZIKV-infected HEK293 cells. Cytotoxicity of IHVR-19029 was assessed and showed a CC_{50} greater than 100 μM (52). These results were similar to our study in which cytotoxicity was not seen up to 100 μM for three of the ER-AGIs tested: castanospermine, Celgosivir and DNJ. Additionally, cytotoxicity was only seen at 1000 μM of NN-DNJ.

ER-AGIs are known to interfere with viral protein synthesis as well as maturation of viral particles (56). While this study did not investigate the mechanism underlying the ability of ER-AGIs to inhibit ZIKV replication, the data is in accordance with the earlier studies. Our results suggest that ER-AGIs act by reducing secretion of infectious virus particles or by secreting particles that are less infectious. We found that ER-AGI treatment resulted in reduced viral RNA and infectious virus in cell culture supernatant compared with control cells suggesting there is less virus particles produced by ER-AGI treated cells

suggesting impaired virus replication. Notably, the reduction in infectious virus titer is much greater than reduction in viral RNA. This observation suggests that there are also defective particles which would indicate inefficient virus maturation in ER-AGI treated cells. It was proposed that viral RNA measured by qRT-PCR that is not accounted for by infectious virus particles, represents viral RNA encapsulated in non-infectious virions (90). The only ER-AGI tested that did not follow this observation was NN-DNJ shown in Figure 3-5. The results of the high-throughput MTS assay show that NN-DNJ increases the cell viability of ZIKV-infected cells from 0.01 to 100 μM at 72 hpi when significant cell death is seen (Figure 3-9D). However, the virus replication analysis done at 48 hpi show no significant reduction in viral RNA or infectious titers in Vero cells (Figure 3-5A and 3-5B). While the exact reasons for the discrepancy is not known, a potential possibility is that the concentration of the compound used and the duration of treatment may have contributed to this effect. The MTS assay measured cell death at 72 hr with multiple concentrations whereas the virus replication was assessed at 48hrs with a 1 μM concentration of NN-DNJ. Hence, it is possible that the reduction in virus replication could be seen much later i.e., at 72h or it may need higher concentration than 1 μM of NN-DNJ to see a difference at 48h. This would allow us to assess if the MTS screening is a true reflection of the antiviral activity of these compounds. Notably, there was a significant reduction of viral RNA at 48hr with 1 μM concentration of NN-DNJ in CHME-3 cells (Figure 3-5C). This highlights that there could be compound specific and cell type specific difference in the efficacy of ER-AGI. Therefore it is important to consider and test various concentrations and timepoints for each compound to determine its individual efficacy.

It is well-known that infection of cells with ZIKV induces upregulation of antiviral genes (91). Our study results also showed that ZIKV infection results in upregulation of key antiviral factors. These antiviral genes include interferon regulatory factor (IRF7), pattern recognition receptors RIGI and MDA5, interferon-simulated genes namely MX-1 and ISG15 and Type I IFN, IFNβ.

We further studied the effect of ER-AGIs on the human microglial cell antiviral response upon ZIKV infection and saw that they have no effect on antiviral gene expression when comparing Celgosivir-treated ZIKV-infected CHME-3 cells to untreated ZIKV-infected cells (Fig. 3-7). The effect of ER-AGIs on uninfected CHME3 cells was also studied. We saw that ER-AGIs do not affect basal expression of antiviral genes (Fig. 3-8). This further confirms the established idea that ER-AGIs antiviral activity is due to their inhibition of α-glucosidase enzymes at the endoplasmic reticulum and excludes the idea that they act by regulating antiviral gene expression.

ZIKV infection is characterized by damaging neurological syndromes such as Guillain-Barre syndrome and microcephaly which are multifactorial disease that still need to be studied in depth. It has been widely demonstrated that ZIKV leads to high levels of neuronal cell death (92, 93). This study has also examined the effect of ER-AGIs on ZIKV cytopathogenicity.

Our preliminary high-throughput screen allowed us to study both cytotoxicity and antiviral activity of compounds efficiently. In a previous study, monocyte-derived macrophages (MDMΦ) did not experience cytotoxicity up to 10000 μM for DNJ and 31.6 μM for NN-DNJ. Additionally, comparison of celgosivir and NN-DNJ showed similar

antiviral activity (90). These results were similar to our study in which three compounds, castanospermine, Celgosivir and DNJ did not induce cytotoxicity up to 100 μM. More moderate cytotoxicity was seen in cells treated with 1000 μM of each compound as assessed by MTS assay. Treatment of cells with 1000 μM of NN-DNJ showed severe toxicity. After determining that ER-AGIs did not induce cytotoxicity at clinically relevant concentrations, our general cytopathogenicity MTS assay showed that ER-AGIs were able to reverse the decrease in metabolic activity and percentage of viable Vero and CHME-3 cells that was caused by ZIKV infection.

Earlier studies have shown that ER-AGIs are able to inhibit replication of DENV regardless of serotype. For example, Rathore et. al. showed that Celgosivir had similar EC_{50} values ranging from 0.22 μM to 0.65 μM against all DENV serotypes (DENV 1-4) (94). Additionally, castanospermine was able to inhibit viral spread and virion secretion by all four serotypes of DENV (95). Since there is only one subtype of ZIKV, we hypothesized that ER-AGIs would cause similar antiviral effects against different ZIKV isolates. The results of this study were in strong support of our hypothesis as a decrease in cytopathogenicity was seen upon addition of castanospermine, Celgosivir and DNJ, regardless of the ZIKV strain used. We further investigated the effect of ER-AGIs on apoptosis and necrosis in CHME-3 cells following ZIKV infection.

We found a significant increase in caspase 3/7 in ZIKV infected CHME-3 cells compared with mock infected cells at 48 hpi and 72 hpi indicating significant activation of apoptosis in virus infected cells. Our findings are in accordance with an earlier report that showed significant activation of caspases in neural progenitor cells at 24 hours after

infection with ZIKV (73). Notably, there was no difference in the levels of caspase 3/7 between Celgosivir and DNJ treated cells, and vehicle treated cells after ZIKV infection. This clearly indicated that ER-AGI treatment has no effect on cellular apoptotic pathways.

A key pathogenicity factor in viral infection is necrosis of virus infected cells which leads to pro-inflammatory response due to the leakage of cellular contents. Our data showed that ZIKV infection of CHME-3 cells results in substantial necrosis as evidenced by significantly elevated LDH levels which indicates that ZIKV infection of neuronal cells results in necrosis *in vitro*. In contrast to our findings, a previous study found that LDH levels in Neuro-2a murine cell lines infected with DENV2 at MOI of 1, are not significantly elevated until 96 hpi (96) indicating the differences in cytopathogenicity between DENV and ZIKV in neuronal cells. Further, we found that celgosivir is able to decrease necrosis induced by ZIKV at 72 hpi which could limit inflammatory responses *in vivo* and help limit the clinical disease associated with ZIKV infection.

Of all four compounds studied, celgosivir is the most promising as evidenced by its ability to reduce viral RNA and infectious virus particles in both Vero and CHME-3 cells at both a MOI of 0.5 and 5 with no effect on cellular apoptosis and antiviral responses. Celgosivir is alkylated on its ring nitrogen which has been shown to be more effective as a chemical target than its parent compound or compounds that have no modification on their ring nitrogen (90). Recently, studies have begun to characterize the effect of Celgosivir for Dengue virus in humans and a recent study showed that Celgosivir was efficacious using a 50 mg/kg dose twice. Additionally, Celgosivir was recently assessed in human trials in which it was administered with an initial loading dose of 400 mg/kg followed by 200 mg/kg

twice daily orally. In contrast to the previous study, it was shown that Celgosivir failed to reduce viral load or fever burden in Dengue virus patients. Other studies have changed the dosing regimen to find an optimal strategy for ER-AGI antivirals *in vivo*. In a mouse model of antibody-enhanced DENV infection, viral RNA was significantly reduced in mice treated with 33.3 mg/kg/dose of Celgosivir. While untreated mice had 10^3 more viral RNA than Celgosivir treated mice, infectious virus production was not significantly decreased in celgosivir-treated mice (90). Other studies must look at Celgosivir efficacy in ZIKV infection and see if discerning dosing regimens will be an issue. However, the results of our study show that Celgosivir may be a promising ER-AGI to treat ZIKV.

Thus far, we have shown here three ER-AGIs that are active against ZIKV in a dose-dependent manner *in vitro*. These results are encouraging and are important as a starting point for further validation *in vivo* mouse model. In conclusion, the results of this study raise a possibility that ER-AGIs may be a promising therapeutic against ZIKV infections.

Conclusions

The rapid geographic spread of ZIKV and the devastating neurological pathogenesis associated with epidemic strains, have made ZIKV an urgent global public health concern. The current lack of antiviral therapeutics and vaccination strategies makes research into novel antivirals a priority. This investigation is centered on exploring the ability of a class iminosugars to inhibit ZIKV replication. The data generated from this study show that ER-AGIs decrease ZIKV replication without affecting other key cellular functions namely antiviral response and apoptosis. ER-AGI treatment significantly reduced ZIKV cytopathogenicity in Vero and human microglial CHME-3 cells. All of these features strongly support the potential antiviral and therapeutic efficacy of three compounds against ZIKV and future *in vivo* studies are warranted. The project also validated the high-throughput cell-based screening assay that could be reliably used to screen novel compound libraries for anti-Zika viral activity.

References

1. Dick GWA, Kitchen SF, Haddow AJ. 1952. Zika Virus (I). Isolations and serological specificity. Transactions of the Royal Society of Tropical Medicine and Hygiene 46:509-520.
2. MacNamara FN. 1954. Zika virus : A report on three cases of human infection during an epidemic of jaundice in Nigeria. Transactions of the Royal Society of Tropical Medicine and Hygiene 48:139-145.
3. Lanciotti RS, Kosoy OL, Laven JJ, Velez JO, Lambert AJ, Johnson AJ, Stanfield SM, Duffy MR. 2008. Genetic and Serologic Properties of Zika Virus Associated with an Epidemic, Yap State, Micronesia, 2007. Emerging Infectious Diseases 14:1232-1239.
4. Foy BD, Kobylinski KC, Foy JLC, Blitvich BJ, Travassos da Rosa A, Haddow AD, Lanciotti RS, Tesh RB. 2011. Probable Non–Vector-borne Transmission of Zika Virus, Colorado, USA. Emerging Infectious Diseases 17:880-882.
5. Vorou R. 2016. Zika virus, vectors, reservoirs, amplifying hosts, and their potential to spread worldwide: what we know and what we should investigate urgently. International Journal of Infectious Diseases 48:85-90.
6. Macnamara FN. 1954. Zika virus: a report on three cases of human infection during an epidemic of jaundice in Nigeria. Trans R Soc Trop Med Hyg 48:139-45.
7. Control ECfD. 2014. Zika virus infection outbreak - The Pacific - 2013-2014. European Centre for Disease Prevention and Control,
8. Zanluca C, Melo VCAd, Mosimann ALP, Santos GIVD, Santos CNDD, Luz K. 2015. First report of autochthonous transmission of Zika virus in Brazil. Memorias do Instituto Oswaldo Cruz 110:569-572.
9. Organization TWH. 2016. Zika virus, Microcephaly and Guillain-Barré syndrome. http://www.who.int/emergencies/zika-virus/situation-report/7-april-2016/en/. Accessed
10. Fauci AS, Morens DM. 2016. Zika Virus in the Americas — Yet Another Arbovirus Threat. New England Journal of Medicine 374:601-604.
11. Prevention CfDCa. 2018. 2017 Case Counts in the US. Centers for Disease Control and Prevention,
12. Prevention CfDCa. 2018. 2018 Case Counts in the US. Centers for Disease Control and Prevention,
13. Prevention CfDCa. 2018. Zika Travel Information. Centers for Disease Control and Prevention,
14. Singh R, Dhama K, Malik Y, Ramakrishnan M, Karthik K, Tiwari R, Saurabh S, Sachan S, Joshi S. 2016. Zika Virus – Emergence, Evolution, Pathology, Diagnosis and Control: Current Global Scenario and Future Perspectives – A Comprehensive Review, vol 36.
15. Bioinformatics SSIo. 2016. ZIKV virion structure and genome organization. SIB Swiss Institute of Bioinformatics.
16. Shang Z, Song H, Shi Y, Qi J, Gao GF. 2018. Crystal Structure of the Capsid Protein from Zika Virus. Journal of Molecular Biology 430:948-962.
17. Dai L, Song J, Lu X, Deng Y-Q, Musyoki Abednego M, Cheng H, Zhang Y, Yuan Y, Song H, Haywood J, Xiao H, Yan J, Shi Y, Qin C-F, Qi J, Gao George F. 2016. Structures of the Zika Virus Envelope Protein and Its Complex with a Flavivirus Broadly Protective Antibody. Cell Host & Microbe 19:696-704.

18. UniProt. 2016. UniProtKB - Q32ZE1 (POLG_ZIKV). http://www.uniprot.org/uniprot/Q32ZE1. Accessed
19. Zhou H, Wang F, Wang H, Chen C, Zhang T, Han X, Wang D, Chen C, Wu C, Xie W, Wang Z, Zhang L, Wang L, Yang H. 2017. The conformational changes of Zika virus methyltransferase upon converting SAM to SAH. Oncotarget 8:14830-14834.
20. Bollati M, Alvarez K, Assenberg R, Baronti C, Canard B, Cook S, Coutard B, Decroly E, de Lamballerie X, Gould EA, Grard G, Grimes JM, Hilgenfeld R, Jansson AM, Malet H, Mancini EJ, Mastrangelo E, Mattevi A, Milani M, Moureau G, Neyts J, Owens RJ, Ren J, Selisko B, Speroni S, Steuber H, Stuart DI, Unge T, Bolognesi M. 2010. Structure and functionality in flavivirus NS-proteins: Perspectives for drug design. Antiviral Research 87:125-148.
21. Aagaard KM, Lahon A, Suter MA, Arya RP, Seferovic MD, Vogt MB, Hu M, Stossi F, Mancini MA, Harris RA, Kahr M, Eppes C, Rac M, Belfort MA, Park CS, Lacorazza D, Rico-Hesse R. 2017. Primary Human Placental Trophoblasts are Permissive for Zika Virus (ZIKV) Replication. Scientific Reports 7:41389.
22. Buckley A, Gould EA. 1988. Detection of Virus-specific Antigen in the Nuclei or Nucleoli of Cells Infected with Zika or Langat Virus. Journal of General Virology 69:1913-1920.
23. Saiz J-C, Vázquez-Calvo Á, Blázquez AB, Merino-Ramos T, Escribano-Romero E, Martín-Acebes MA. 2016. Zika Virus: the Latest Newcomer. Frontiers in Microbiology 7:496.
24. Meertens L, Labeau A, Dejarnac O, Cipriani S, Sinigaglia L, Bonnet-Madin L, Le Charpentier T, Hafirassou ML, Zamborlini A, Cao-Lormeau V-M, Coulpier M, Missé D, Jouvenet N, Tabibiazar R, Gressens P, Schwartz O, Amara A. Axl Mediates ZIKA Virus Entry in Human Glial Cells and Modulates Innate Immune Responses. Cell Reports 18:324-333.
25. Perera R, Khaliq M, Kuhn RJ. 2008. Closing the door on flaviviruses: Entry as a target for antiviral drug design. Antiviral Research 80:11-22.
26. Prevention CfDCa. 2017. Men and Zika.
27. Gould E, Pettersson J, Higgs S, Charrel R, de Lamballerie X. 2017. Emerging arboviruses: Why today? One Health 4:1-13.
28. Velasquez-Serra GC. 2016. Zika Virus Vectors. American Journal of Epidemiology and Infectious Disease 4:78-83.
29. Weger-Lucarelli J, Rückert C, Chotiwan N, Nguyen C, Garcia Luna SM, Fauver JR, Foy BD, Perera R, Black WC, Kading RC, Ebel GD. 2016. Vector Competence of American Mosquitoes for Three Strains of Zika Virus. PLOS Neglected Tropical Diseases 10:e0005101.
30. Althouse BM, Vasilakis N, Sall AA, Diallo M, Weaver SC, Hanley KA. 2016. Potential for Zika Virus to Establish a Sylvatic Transmission Cycle in the Americas. PLOS Neglected Tropical Diseases 10:e0005055.
31. Musso D, Nhan T, Robin E, Roche C, Bierlaire D, Zisou K, Shan Yan A, Cao-Lormeau VM, Broult J. 2014. Potential for Zika virus transmission through blood transfusion demonstrated during an outbreak in French Polynesia, November 2013 to February 2014. Eurosurveillance 19:20761.
32. Elisabeth RK-L, Brad JB, Staples JE. 2017. Estimated Incubation Period for Zika Virus Disease. Emerging Infectious Disease journal 23:841.
33. Musso D, Gubler DJ. 2016. Zika Virus. Clin Microbiol Rev 29:487-524.

34. Miner Jonathan J, Diamond Michael S. 2016. Understanding How Zika Virus Enters and Infects Neural Target Cells. Cell Stem Cell 18:559-560.
35. Petersen LR, Jamieson DJ, Powers AM, Honein MA. 2016. Zika Virus. New England Journal of Medicine 374:1552-1563.
36. Noronha Ld, Zanluca C, Azevedo MLV, Luz KG, Santos CNDd. 2016. Zika virus damages the human placental barrier and presents marked fetal neurotropism. Memórias do Instituto Oswaldo Cruz 111:287-293.
37. Quicke Kendra M, Bowen James R, Johnson Erica L, McDonald Circe E, Ma H, O'Neal Justin T, Rajakumar A, Wrammert J, Rimawi Bassam H, Pulendran B, Schinazi Raymond F, Chakraborty R, Suthar Mehul S. 2016. Zika Virus Infects Human Placental Macrophages. Cell Host & Microbe 20:83-90.
38. Tang H, Hammack C, Ogden Sarah C, Wen Z, Qian X, Li Y, Yao B, Shin J, Zhang F, Lee Emily M, Christian Kimberly M, Didier Ruth A, Jin P, Song H, Ming G-l. 2016. Zika Virus Infects Human Cortical Neural Progenitors and Attenuates Their Growth. Cell Stem Cell 18:587-590.
39. Retallack H, Di Lullo E, Arias C, Knopp KA, Laurie MT, Sandoval-Espinosa C, Mancia Leon WR, Krencik R, Ullian EM, Spatazza J, Pollen AA, Mandel-Brehm C, Nowakowski TJ, Kriegstein AR, DeRisi JL. 2016. Zika virus cell tropism in the developing human brain and inhibition by azithromycin. Proceedings of the National Academy of Sciences 113:14408.
40. Sheridan MA, Balaraman V, Schust DJ, Ezashi T, Roberts RM, Franz AWE. 2018. African and Asian strains of Zika virus differ in their ability to infect and lyse primitive human placental trophoblast. PLOS ONE 13:e0200086.
41. Zhu Z, Chan JF-W, Tee K-M, Choi GK-Y, Lau SK-P, Woo PC-Y, Tse H, Yuen K-Y. 2016. Comparative genomic analysis of pre-epidemic and epidemic Zika virus strains for virological factors potentially associated with the rapidly expanding epidemic. Emerging Microbes &Amp; Infections 5:e22.
42. Culshaw A, Mongkolsapaya J, Screaton G. 2018. The immunology of Zika Virus. F1000Research 7:203.
43. Organization WH. 2017. Mosquito control: can it stop Zika at source? World Health Organization,
44. von Seidlein L, Kekulé AS, Strickman D. 2017. Novel Vector Control Approaches: The Future for Prevention of Zika Virus Transmission? PLOS Medicine 14:e1002219.
45. Poland GA, Kennedy RB, Ovsyannikova IG, Palacios R, Ho PL, Kalil J. 2018. Development of vaccines against Zika virus. The Lancet Infectious Diseases 18:e211-e219.
46. Khandia R, Munjal A, Dhama K, Karthik K, Tiwari R, Malik YS, Singh RK, Chaicumpa W. 2018. Modulation of Dengue/Zika Virus Pathogenicity by Antibody-Dependent Enhancement and Strategies to Protect Against Enhancement in Zika Virus Infection. Frontiers in Immunology 9:597.
47. Richard AS, Shim B-S, Kwon Y-C, Zhang R, Otsuka Y, Schmitt K, Berri F, Diamond MS, Choe H. 2017. AXL-dependent infection of human fetal endothelial cells distinguishes Zika virus from other pathogenic flaviviruses. Proceedings of the National Academy of Sciences 114:2024-2029.
48. Sacramento CQ, de Melo GR, de Freitas CS, Rocha N, Hoelz LVB, Miranda M, Fintelman-Rodrigues N, Marttorelli A, Ferreira AC, Barbosa-Lima G, Abrantes JL, Vieira YR, Bastos MM, de Mello Volotão E, Nunes EP, Tschoeke DA, Leomil L, Loiola EC, Trindade P, Rehen SK, Bozza FA, Bozza PT, Boechat N, Thompson FL, de Filippis

AMB, Brüning K, Souza TML. 2017. The clinically approved antiviral drug sofosbuvir inhibits Zika virus replication. Scientific Reports 7:40920.
49. Pires de Mello CP, Tao X, Kim TH, Vicchiarelli M, Bulitta JB, Kaushik A, Brown AN. 2018. Clinical Regimens of Favipiravir Inhibit Zika Virus Replication in the Hollow-Fiber Infection Model. Antimicrobial Agents and Chemotherapy 62.
50. Wu S-F, Lee C-J, Liao C-L, Dwek RA, Zitzmann N, Lin Y-L. 2002. Antiviral Effects of an Iminosugar Derivative on Flavivirus Infections. Journal of Virology 76:3596-3604.
51. Chang J, Block TM, Guo J-T. 2013. Antiviral therapies targeting host ER alpha-glucosidases: Current status and future directions. Antiviral Research 99:251-260.
52. Ma J, Zhang X, Soloveva V, Warren T, Guo F, Wu S, Lu H, Guo J, Su Q, Shen H, Solon E, Comunale MA, Mehta A, Guo J-T, Bavari S, Du Y, Block TM, Chang J. 2018. Enhancing the antiviral potency of ER α-glucosidase inhibitor IHVR-19029 against hemorrhagic fever viruses in vitro and in vivo. Antiviral Research 150:112-122.
53. Alonzi DS, Scott KA, Dwek RA, Zitzmann N. 2017. Iminosugar antivirals: the therapeutic sweet spot. Biochemical Society Transactions 45:571-582.
54. Sadat MA, Moir S, Chun T-W, Lusso P, Kaplan G, Wolfe L, Memoli MJ, He M, Vega H, Kim LJY, Huang Y, Hussein N, Nievas E, Mitchell R, Garofalo M, Louie A, Ireland DC, Grunes C, Cimbro R, Patel V, Holzapfel G, Salahuddin D, Bristol T, Adams D, Marciano BE, Hegde M, Li Y, Calvo KR, Stoddard J, Justement JS, Jacques J, Priel DAL, Murray D, Sun P, Kuhns DB, Boerkoel CF, Chiorini JA, Di Pasquale G, Verthelyi D, Rosenzweig SD. 2014. Glycosylation, hypogammaglobulinemia, and resistance to viral infections. The New England journal of medicine 370:1615-1625.
55. Chang J, Warren TK, Zhao X, Gill T, Guo F, Wang L, Comunale MA, Du Y, Alonzi DS, Yu W, Ye H, Liu F, Guo J-T, Mehta A, Cuconati A, Butters TD, Bavari S, Xu X, Block TM. 2013. Small molecule inhibitors of ER α-glucosidases are active against multiple hemorrhagic fever viruses. Antiviral research 98:432-440.
56. Chang J, Guo J-T, Du Y, Block T. 2013. Imino sugar glucosidase inhibitors as broadly active anti-filovirus agents. Emerging Microbes &Amp; Infections 2:e77.
57. Perry ST, Buck MD, Plummer EM, Penmasta RA, Batra H, Stavale EJ, Warfield KL, Dwek RA, Butters TD, Alonzi DS, Lada SM, King K, Klose B, Ramstedt U, Shresta S. 2013. An iminosugar with potent inhibition of dengue virus infection in vivo. Antiviral Research 98:35-43.
58. Reed LJ, Muench H. 1938. A SIMPLE METHOD OF ESTIMATING FIFTY PER CENT ENDPOINTS12. American Journal of Epidemiology 27:493-497.
59. Thomas Fletcher III RP, Stacy Bartram, Susan Halliday, Robert Buckheit, Jr.,Rich Moravec, and Terry Riss. A High-Throughput System for Screening Potential Antiviral Compounds Using the CellTiter 96® AQueous One Solution Assay. Promega,
60. Goebel S, Snyder B, Sellati T, Saeed M, Ptak R, Murray M, Bostwick R, Rayner J, Koide F, Kalkeri R. 2016. A sensitive virus yield assay for evaluation of Antivirals against Zika Virus. Journal of Virological Methods 238:13-20.
61. Kuchipudi SV, Tellabati M, Nelli RK, White GA, Perez BB, Sebastian S, Slomka MJ, Brookes SM, Brown IH, Dunham SP, Chang K-C. 2012. 18S rRNA is a reliable normalisation gene for real time PCR based on influenza virus infected cells. Virology journal 9:230-230.
62. Pauli E-K, Schmolke M, Wolff T, Viemann D, Roth J, Bode JG, Ludwig S. 2008. Influenza A Virus Inhibits Type I IFN Signaling via NF-κB-Dependent Induction of SOCS-3 Expression. PLOS Pathogens 4:e1000196.

63. Liu L-L, Zhao H, Ma T-F, Ge F, Chen C-S, Zhang Y-P. 2015. Identification of Valid Reference Genes for the Normalization of RT-qPCR Expression Studies in Human Breast Cancer Cell Lines Treated with and without Transient Transfection. PLoS ONE 10:e0117058.
64. Hildyard JC, Wells DJ. 2014. Identification and validation of quantitative PCR reference genes suitable for normalizing expression in normal and dystrophic cell culture models of myogenesis. PLoS Curr 6.
65. Seng L-G, Daly J, Chang K-C, Kuchipudi SV. 2014. High Basal Expression of Interferon-Stimulated Genes in Human Bronchial Epithelial (BEAS-2B) Cells Contributes to Influenza A Virus Resistance. PLoS ONE 9:e109023.
66. Livingstone M, Sikström K, Robert PA, Uzé G, Larsson O, Pellegrini S. 2015. Assessment of mTOR-Dependent Translational Regulation of Interferon Stimulated Genes. PLOS ONE 10:e0133482.
67. Kim M-J, Hwang S-Y, Imaizumi T, Yoo J-Y. 2008. Negative Feedback Regulation of RIG-I-Mediated Antiviral Signaling by Interferon-Induced ISG15 Conjugation. Journal of Virology 82:1474-1483.
68. Nasirudeen AMA, Wong HH, Thien P, Xu S, Lam K-P, Liu DX. 2011. RIG-I, MDA5 and TLR3 Synergistically Play an Important Role in Restriction of Dengue Virus Infection. PLOS Neglected Tropical Diseases 5:e926.
69. Muramatsu D, Kawata K, Aoki S, Uchiyama H, Okabe M, Miyazaki T, Kida H, Iwai A. 2014. Stimulation with the Aureobasidium pullulans-produced β-glucan effectively induces interferon stimulated genes in macrophage-like cell lines. Scientific Reports 4:4777.
70. Megiorni F, Indovina P, Mora B, Mazzilli MC. 2005. Minor expression of fascin-1 gene (FSCN1) in NTera2 cells depleted of CREB-binding protein. Neuroscience Letters 381:169-174.
71. Arena A, Bisignano G, Pavone B, Tomaino A, Bonina FP, Saija A, Cristani M, D'Arrigo M, Trombetta D. 2008. Antiviral and immunomodulatory effect of a lyophilized extract of Capparis spinosa L. buds. Phytother Res 22:313-7.
72. Zhao X, Cui Q, Fu Q, Song X, Jia R, Yang Y, Zou Y, Li L, He C, Liang X, Yin L, Lin J, Ye G, Shu G, Zhao L, Shi F, Lv C, Yin Z. 2017. Antiviral properties of resveratrol against pseudorabies virus are associated with the inhibition of IκB kinase activation. Scientific Reports 7:8782.
73. Souza BSF, Sampaio GLA, Pereira CS, Campos GS, Sardi SI, Freitas LAR, Figueira CP, Paredes BD, Nonaka CKV, Azevedo CM, Rocha VPC, Bandeira AC, Mendez-Otero R, dos Santos RR, Soares MBP. 2016. Zika virus infection induces mitosis abnormalities and apoptotic cell death of human neural progenitor cells. Scientific Reports 6:39775.
74. Russo FB, Beltrao-Braga PCB. 2017. The impact of Zika virus in the brain. Biochem Biophys Res Commun 492:603-607.
75. Wen Z, Song H, Ming G-l. 2017. How does Zika virus cause microcephaly? Genes & Development 31:849-861.
76. Manangeeswaran M, Ireland DD, Verthelyi D. 2016. Zika (PRVABC59) Infection Is Associated with T cell Infiltration and Neurodegeneration in CNS of Immunocompetent Neonatal C57Bl/6 Mice. PLoS Pathog 12:e1006004.
77. Yuan L, Huang XY, Liu ZY, Zhang F, Zhu XL, Yu JY, Ji X, Xu YP, Li G, Li C, Wang HJ, Deng YQ, Wu M, Cheng ML, Ye Q, Xie DY, Li XF, Wang X, Shi W, Hu B, Shi PY, Xu Z, Qin CF. 2017. A single mutation in the prM protein of Zika virus contributes to fetal microcephaly. Science 358:933-936.

78. Tiwari SK, Dang J, Qin Y, Lichinchi G, Bansal V, Rana TM. 2017. Zika virus infection reprograms global transcription of host cells to allow sustained infection. Emerg Microbes Infect 6:e24.
79. Swartwout B, Zlotnick M, Saver A, McKenna C, Bertke A. 2017. Zika Virus Persistently and Productively Infects Primary Adult Sensory Neurons In Vitro. Pathogens 6:49.
80. Papa MP, Meuren LM, Coelho SVA, Lucas CGdO, Mustafá YM, Lemos Matassoli F, Silveira PP, Frost PS, Pezzuto P, Ribeiro MR, Tanuri A, Nogueira ML, Campanati L, Bozza MT, Paula Neto HA, Pimentel-Coelho PM, Figueiredo CP, Aguiar RSd, Arruda LBd. 2017. Zika Virus Infects, Activates, and Crosses Brain Microvascular Endothelial Cells, without Barrier Disruption. Frontiers in Microbiology 8.
81. Roosecelis Brasil Martines JB, M. Kelly Keating, Luciana Silva-Flannery, Atis Muehlenbachs, Joy Gary, Cynthia Goldsmith, Gillian Hale, Jana Ritter, Dominique Rollin, Wun-Ju Shieh, Kleber G. Luz, Ana Maria de Oliveira Ramos, Helaine Pompeia Freire Davi, Wanderson Kleber de Oliveria, Robert Lanciotti, Amy Lambert, Amy Lambert. 2016. Notes from the Field: Evidence of Zika Virus Infection in Brain and Placental Tissues from Two Congenitally Infected Newborns and Two Fetal Losses — Brazil, 2015. Centers for Disease Control and Prevention,
82. Simsek E, Lu X, Ouzounov S, Block TM, Mehta AS. 2006. α-Glucosidase Inhibitors Have a Prolonged Antiviral Effect against Hepatitis B Virus through the Sustained Inhibition of the Large and Middle Envelope Glycoproteins. Antiviral Chemistry and Chemotherapy 17:259-267.
83. Gu B, Mason P, Wang L, Norton P, Bourne N, Moriarty R, Mehta A, Despande M, Shah R, Block T. 2007. Antiviral Profiles of Novel Iminocyclitol Compounds against Bovine Viral Diarrhea Virus, West Nile Virus, Dengue Virus and Hepatitis B Virus. Antiviral Chemistry and Chemotherapy 18:49-59.
84. Qu X, Pan X, Weidner J, Yu W, Alonzi D, Xu X, Butters T, Block T, Guo J-T, Chang J. 2011. Inhibitors of Endoplasmic Reticulum α-Glucosidases Potently Suppress Hepatitis C Virus Virion Assembly and Release. Antimicrobial Agents and Chemotherapy 55:1036-1044.
85. Fischl MA, Resniek L, Coombs R, Kremer AB, Pottage JCJ, Fass RJ, Fife KH, Powderly WG, Collier AC, Aspinall RL, Smith SL, Kowalski KG, Wallemark C-B. 1994. The Safety and Efficacy of Combination N-Butyl-Deoxynojirimycin (SC-48334) and Zidovudine in Patients with HIV-1 Infection and 200–500 CD4 Cells/mm. JAIDS Journal of Acquired Immune Deficiency Syndromes 7:139-147.
86. Schlesinger S, Koyama AH, Malfer C, Gee SL, Schlesinger MJ. 1985. The effects of inhibitors of glucosidase I on the formation of Sindbis virus. Virus Research 2:139-149.
87. Taylor DL, Fellows LE, Farrar GH, Nash RJ, Taylor-Robinson D, Mobberley MA, Ryder TA, Jeffries DJ, Tyms AS. 1988. Loss of cytomegalovirus infectivity after treatment with castanospermine or related plant alkaloids correlates with aberrant glycoprotein synthesis. Antiviral Research 10:11-26.
88. Datema R, Olofsson S, Romero PA. 1987. Inhibitors of protein glycosylation and glycoprotein processing in viral systems. Pharmacology & Therapeutics 33:221-286.
89. Kim SY, Li B, Linhardt RJ. 2017. Pathogenesis and Inhibition of Flaviviruses from a Carbohydrate Perspective. Pharmaceuticals (Basel) 10.
90. Sayce AC, Alonzi DS, Killingbeck SS, Tyrrell BE, Hill ML, Caputo AT, Iwaki R, Kinami K, Ide D, Kiappes JL, Beatty PR, Kato A, Harris E, Dwek RA, Miller JL, Zitzmann N. 2016. Iminosugars Inhibit Dengue Virus Production via Inhibition of ER

Alpha-Glucosidases—Not Glycolipid Processing Enzymes. PLOS Neglected Tropical Diseases 10:e0004524.
91. Carlin AF, Vizcarra EA, Branche E, Viramontes KM, Suarez-Amaran L, Ley K, Heinz S, Benner C, Shresta S, Glass CK. 2018. Deconvolution of pro- and antiviral genomic responses in Zika virus-infected and bystander macrophages. Proceedings of the National Academy of Sciences doi:10.1073/pnas.1807690115.
92. Costa VV, Del Sarto JL, Rocha RF, Silva FR, Doria JG, Olmo IG, Marques RE, Queiroz-Junior CM, Foureaux G, Araújo JMS, Cramer A, Real ALCV, Ribeiro LS, Sardi SI, Ferreira AJ, Machado FS, de Oliveira AC, Teixeira AL, Nakaya HI, Souza DG, Ribeiro FM, Teixeira MM. 2017. N-Methyl-d-Aspartate (NMDA) Receptor Blockade Prevents Neuronal Death Induced by Zika Virus Infection. mBio 8:e00350-17.
93. Olmo IG, Carvalho TG, Costa VV, Alves-Silva J, Ferrari CZ, Izidoro-Toledo TC, da Silva JF, Teixeira AL, Souza DG, Marques JT, Teixeira MM, Vieira LB, Ribeiro FM. 2017. Zika Virus Promotes Neuronal Cell Death in a Non-Cell Autonomous Manner by Triggering the Release of Neurotoxic Factors. Frontiers in Immunology 8:1016.
94. Rathore APS, Paradkar PN, Watanabe S, Tan KH, Sung C, Connolly JE, Low J, Ooi EE, Vasudevan SG. 2011. Celgosivir treatment misfolds dengue virus NS1 protein, induces cellular pro-survival genes and protects against lethal challenge mouse model. Antiviral Research 92:453-460.
95. Whitby K, Pierson TC, Geiss B, Lane K, Engle M, Zhou Y, Doms RW, Diamond MS. 2005. Castanospermine, a potent inhibitor of dengue virus infection in vitro and in vivo. J Virol 79:8698-706.
96. Ho M-R, Tsai T-T, Chen C-L, Jhan M-K, Tsai C-C, Lee Y-C, Chen C-H, Lin C-F. 2017. Blockade of dengue virus infection and viral cytotoxicity in neuronal cells in vitro and in vivo by targeting endocytic pathways. Scientific Reports 7:6910.